Volume 10, Issue 2, 2020, 5096 - 5116 ISSN 2069-5837
Biointerface Research in Applied Chemistry
www.BiointerfaceResearch.com
https://doi.org/10.33263/BRIAC102.096116
Original Research Article Open Access Journal
Received: 12.01.2020 / Revised: 23.01.2020 / Accepted: 24.01.2020 / Published on-line: 28.01.2020

DFT study of species derived from the narcotic antagonist naloxone

María Jimena Márquez [1], Silvia Antonia Brandán [1,*]

[1]Cátedra de Química General, Instituto de Química Inorgánica, Facultad de Bioquímica. Química y Farmacia, Universidad Nacional de Tucumán, Ayacucho 471, (4000) San Miguel de Tucumán, Tucumán, Argentina

*corresponding author e-mail address: ***sbrandan@fbqf.unt.edu.ar*** | Scopus ID 6602262428

ABSTRACT

The functional hybrid B3LYP and the 6-31G* basis set have been employed to study the theoretical structures of free base, cationic and hydrochloride species of naloxone in gas phase and in aqueous solution. The SCRF methodology and the PCM method were used to optimize the species in solution while the solvation energies were computed with the universal solvation model. The harmonic force fields of three species in the two media were computed with the SQMFF methodology and the Molvib program while the complete vibrational assignments of bands observed in the experimental available ATR and Raman spectra were performed by using the harmonic force fields and the normal internal coordinates. Therefore, the expected 129, 132 and 135 vibration normal modes for the free base, cationic and hydrochloride species of naloxone, respectively are here reported. The free base of naloxone evidence the higher solvation energy value, as compared with those reported for S(-)-promethazine, R(+)-promethazine, cyclizine, morphine, cocaine, scopolamine, heroin, and tropane alkaloids. The cationic species shows a solvation energy value (-302.45 kJ/mol) closer to observed for morphine (-309.19 kJ/mol) while the value for the hydrochloride species (-122.28 kJ/mol) is near to scopolamine value (-122.74 kJ/mol). AIM analyses show ionic characteristic of N-H···Cl bonds in the hydrochloride species and suggest that this species in both media is as cationic one, as supported by the positive MK charges on the N5 atoms in the hydrochloride species in both media and by the absence in the ATR spectrum of band at 2405 cm^{-1}, associated to N5-H46 stretching mode. Moreover, frontier orbitals studies evidence that the allyl chains present in the three species of naloxone diminishing the gap values increasing their reactivities, as compared with the other species containing the N-CH_3 group. The *f(νN-H)* force constants for the hydrochloride species is lower than the corresponding in solution, a result also observed for morphine (2.73 and 4.61 mdyn $Å^{-1}$), cocaine (3.23 and 4.79 mdyn $Å^{-1}$) and tropane (2.70 and 4.69 mdyn $Å^{-1}$) alkaloids. Comparisons between experimental infrared, Raman and ultraviolet-visible spectra with the corresponding predicted show good correlations.

Keywords: *Naloxone; Force fields; Vibrational analysis; DFT calculations; Molecular structure.*

1. INTRODUCTION

DFT calculations are very useful tools to analyse structures and predict properties of numerous compounds with different fused rings [1-15], such as tropane alkaloids. These alkaloids contain the >N-CH_3 group and present a wide range of biological properties and different structural, electronic and topological properties some of which were studied by our research group [1-7]. In the free base, cationic and hydrochloride species of these alkaloids can be observed a N atom tertiary where the N-C distance plays a very important role in the stability of species and where changes in the charges, in the electronic densities of rings, stabilization and solvation energies were detected when the >N-CH_3 group is linked to fused or alone rings [7]. Besides, the >N-CH_3 group can be present in other species that present antihistaminic properties, as in promethazine, diphenidramine and cyclizine [8,16,17]. On the other hand, the studies in solution have revealed that in the solid phase and in aqueous solution the hydrochloride/hydrobromide form is clearly present as cationic one, as suggested by its infrared and Raman spectra [1-3,5-8,16,17]. In this work, the structures and properties of naloxone narcotic agent were studied combining DFT calculations with experimental data because in this species the N atom tertiary is linked to allyl >N-CH_2-CH=CH_2 group different from the N-CH_3 group. So far, for that narcotic antagonist containing five fused rings similar to morphine alkaloid the structural, electronic, topological and vibrational properties were not reported. The importance of this study is due to that naloxone hydrochloride species is the narcotic agent antagonist used in the treatment caused by overdoses of heroin, morphine or other opioids. Thus, naloxone hydrochloride acts blocking the receptor sites and, this way, reverses the effects of the narcotic agonist [18-20]. Some synonyms of naloxone are n-allylnoroxymorphone and narcan while its IUPAC name is (4*R*,4*aS*,7*aR*,12*bS*)-4*a*,9-dihydroxy-3-prop-2-enyl-2,4,5,6,7*a*,13-hexahydro-1*H*-4,12-methanobenzofuro[3,2-e]isoquinolin-7-one. The experimental structure of naloxone hydrochloride was determined by X-ray diffraction by Karle whose has reported that the conformation of the ring system in naloxone is similar to that in morphine and codeine [21]. Here, the structures of free base, cationic and hydrochloride species of naloxone were modelled and optimized by using the functional hybrid B3LYP/6-31G* in gas and aqueous solution [22,23]. The calculations in solution were performed with the integral equation formalism variant polarised continuum method (IEFPCM) and universal solvation model [24-26]. Besides, the scaled quantum mechanical force field (SQMFF) method and the Molvib program [27-29] were employed to perform the complete vibrational assignments of its experimental available infrared, attenuated total reflectance (ATR) and Raman spectra [30]. Reactivities and behaviours of three species of naloxone were also predicted by using the frontier orbitals and equations available from the literature [31-40]. The predicted

properties for naloxone in both media were compared with those published for other alkaloids [1-7].

2. MATERIALS AND METHODS

The free base, cationic and hydrochloride structures of naloxone were modelled with the *GaussView* program [41] adding first an H atom to the free base and, then, to it a Cl atom. The optimizations of these three structures were performed in gas phase and aqueous solution with the Revision A.02 of Gaussian program [42] and the functional hybrid B3LYP/6-31G* method [22,23]. Particularly, in solution both IEFPCM and universal solvation methods were used because these schemes consider the solvent effects [24-26]. The optimized theoretical molecular structures of free base, cationic and hydrocloride species of naloxone in gas phase by using the B3LYP/6-31G* method can be seen in **Figure 1** together with atoms labelling and identification of their rings. The volumes and its variations were calculated with the Moldraw program [43]. The natures of the reached stationary points for those three structures were checked with the vibrational frequencies. The atomic charges, molecular electrostatic potentials, bond orders and topological properties were obtained with the versions 3.2 of NBO and AIM2000 programs [44,45] while the frontier orbitals and some descriptors [31-40] were used to predict kinetics stabilities, reactivities and behaviours in both media. Vibrational analyses for the three species of naloxone were performed computing the harmonic force fields with the scaled mechanical force field (SQMFF) methodology and the version 7.0 of Molvib program [27-29] by using the normal internal coordinates and transferable scaling factors. Then, the complete assignments of bands observed in the experimental available infrared and Raman spectra of hydrochloride species of naloxone were performed by using the corresponding harmonic force fields and considering potential energy distribution (PED) contributions ≥ 5 % in the region of lower wavenumbers. Finally, the Time-dependent DFT calculations (TD-DFT) were used to predict the ultraviolet-visible spectra of three species of naloxone in aqueous solution at the same level of theory with the Gaussian 09 program [42].

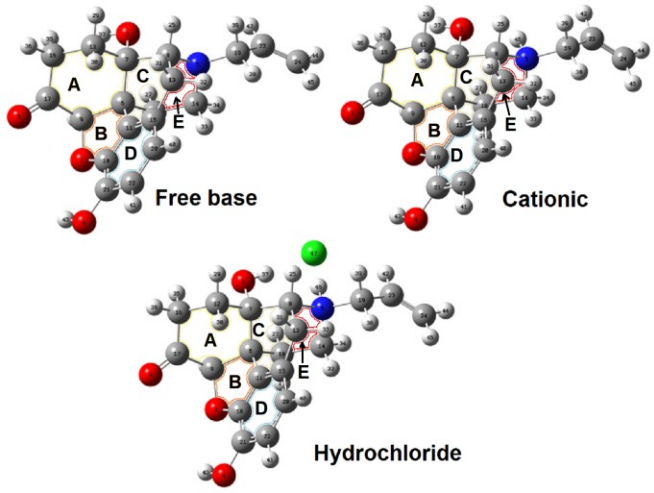

Figure 1. Theoretical molecular structures of free base, cationic and hydrocloride species of naloxone, atoms labelling and identification of their rings.

3. RESULTS

Structures in both media and solvation energies.

In **Figure 1** are presented the optimized theoretical structures of free base, cationic and hydrocloride species of naloxone in gas phase by using the B3LYP/6-31G* method together with atoms labelling and identification of their rings. The three structures of naloxone were optimized with C_1 symmetries.

Table 1. Calculated total energies (*E*), dipole moments (μ) and volumes (V) of three species of naloxone in gas and aqueous solution phases.

B3LYP/6-31G* Method					
Medium	E (Hartrees)	ZPVE	μ (D)	V (Å^3)	ΔV (Å^3)
Free base					
GAS	-1092.2452	-1091.8716	2.84	334.3	-1.5
PCM	-1092.2756	-1091.9012	4.20	332.8	
Cationic					
GAS	-1092.6459	-1092.2567	10.81	337.4	-2.6
PCM	-1092.7498	-1092.3595	15.48	334.8	
Hydrochloride					
GAS	-1553.0793	-1552.6903	7.21	361.2	-0.1
PCM	-1553.1171	-1552.7270	10.87	361.1	

The fused A, C, D and E rings are of members six while only the B ring is of five members. The ring system in the hydrocloride species of naloxone is similar to morphine, as was experimentally observed by Karle [21]. The total energy corrected by ZPVE, moment dipolar, volume and volume variations values for the three species of naloxone in both media by using the functional hybrid B3LYP/6-31G* method is observed in **Table 1**. These results have evidenced that all species in gas phase present low dipole moments values, as compared with the corresponding values in solution. However, the calculations predict low volumes values in solution and, hence, volumes contractions for the three species of naloxone are observed in this medium. The higher value it is observed for the cationic species, as expected, taking into account that this species presents the higher dipole moment value in both media, especially in solution. Note that the total energy presents lower values when these are corrected by ZPVE.

In **Table 2** are presented solvation energy values corrected and uncorrected by the total non-electrostatic terms and by zero point vibrational energy (ZPVE) for the three species of naloxone in aqueous solution by using the functional hybrid B3LYP/6-31G* method.

Table 2. Corrected and uncorrected solvation energies by the total non-electrostatic terms and by zero point vibrational energy (ZPVE) of three species of naloxone by using the B3LYP/6-31G* method compared with other species.

B3LYP/6-31G* method[a]			
Solvation energy (kJ/mol)			
Condition	$\Delta G_{un}^{\#}$	ΔG_{ne}	ΔG_c
Free base			
Naloxone[a]	-77.64	23.11	-100.75
S(-)-Promethazine[b]	-20.19	15.88	-36.07

B3LYP/6-31G* method[a]			
R(+)-Promethazine[b]	-3.41	14.46	-17.87
Cyclizine[c]	-23.60	5.93	-29.53
Morphine[d]	-47.74	13.17	-60.91
Cocaine[e]	-42.75	28.51	-71.26
Scopolamine[f]	-56.66	18.81	-75.47
Heroin[g]	-59.54	29.13	-88.67
Tropane[b,h]	-11.80	0.75	-12.55
Cationic			
Naloxone[a]	-269.64	32.81	-302.45
S(-)-Promethazine[b]	-7.08	7.40	-14.48
R(+)-Promethazine[b]	-255.22	7.59	-262.81
Cyclizine[c,#]	-238.43	5.93	-244.36
Morphine[d]	-282.23	26.96	-309.19
Cocaine[e]	-216.66	38.58	-255.24
Scopolamine[f]	-279.87	30.47	-310.34
Heroin[g]	-280.13	43.01	-323.14
Tropane[b,h]	-228.99	15.34	-244.33
Hydrochloride			
Naloxone[a]	-89.18	33.10	-122.28
S(-)-Promethazine[b]	-101.25	30.81	-70.44
R(+)-Promethazine[b]	-21.51	30.51	-52.02
Cyclizine[c]	-81.57	23.49	-105.06
Morphine[d]	-118.82	25.92	-144.74
Cocaine[e]	-99.94	38.20	-138.14
Scopolamine[f,γ]	-95.19	27.55	-122.74
Heroin[g]	-118.56	43.38	-161.94
Tropane[b,h]	-72.13	15.05	-87.18

ΔG_{un} [#]= uncorrected solvation energy, ΔG_{un} = Solvation energy (kJ/mol) corrected by ZPVE, ΔG_{ne}= total non-electrostatic terms due to the cavitation, dispersion and repulsion energies, ΔG_c= corrected solvation energies, [a]This work, [b]From Ref [8], [c]From Ref [17], [d]From Ref [1], [e]From Ref [3], [f]From Ref [7], [g]From Ref [5], [h]From Ref [2], [#]Cation cyclizine: 6-31+G*, [γ]Hydrobromide.

The corrected solvation energy values are compared with those reported for some alkaloids [1-3,5,7] and for antihistaminic species [8,17]. The behaviours of all species in both media are given in **Figure 2**.

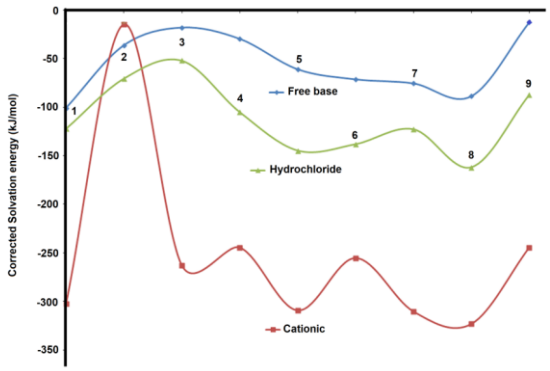

Figure 2. Corrected solvation energies of three species of naloxone (1) by using the B3LYP/6-31G* method compared with the corresponding to S(-)-Promethazine (2) and R(+)-Promethazine (3) [8], Cyclizine (4) [17], Morphine (5) [1], Cocaine (6) [3], Scopolamine (7) [7], Heroin (8) [5] and Tropane (9) [2].

The numbers that identify each compound are presented in the corresponding caption. Analyzing exhaustively the table's values and Figure 2 we observed that both free base and hydrochloride species present the same behaviours in solution although all hydrochloride species present higher solvation energy values than the free base ones. On the other side, the cationic forms of all species have the highest values because in solution the hydrochloride species are present as cationic ones. When the values for the three species of naloxone are compared with the other ones, it is observed that its free base presents the highest value (-100.75 kJ/mol) while the value of its cationic species (-302.45 kJ/mol) is similar to the value observed for morphine (-309.19 kJ/mol). This approximation could be clearly justified with the experimental structure determined by Karle because this author has reported that the ring system in the hydrocloride species of naloxone is similar to the morphine one [21]. Other very important result is that the solvation energy predicted for the hydrochloride species of naloxone (-122.28 kJ/mol) is practically the same than the value corresponding to hydrobromide scopolamine (-122.74 kJ/mol). The hydrochloride species of morphine (-144.74 kJ/mol) presents a value slightly higher than the observed for the same species of naloxone. These differences could be attributed to the different anions present in each species where scopolamine is as hydrobromide different from the other compounds [7]. The lowest solvation energy value for the free base species is observed for the tropane alkaloid while the cationic species of S(-) form of promethazine and the hydrochloride species of R(+) form of promethazine present the lowest values, respectively.

Geometrical parameters in both media.

To carry out the vibrational analyses of all naloxone species it is necessary first to found the most stable structures that generate the lower root-mean-square deviation (RMSD) values when the calculated geometrical parameters for each species of naloxone are compared with the corresponding experimental ones. Then, with these better structures will be calculated the harmonic force fields. For those reasons, in **Table 3** are summarized the calculated bond lengths and angles parameters of three species of naloxone in both media by using the 6-31G* level of theory compared with the experimental ones corresponding to free base and hydrochloride species of morphine [1,46-48]. These comparisons were performed because the bond lengths and angles of rings A, B and C in naloxone are identical chemically to the ring's morphine, as was observed by Karle [21]. Hence, reasonable correlations were found for those two parameters, with values between 0.073 and 0.068 Å for bond lengths and between 7.2 and 1.3 º for bond angles. Higher differences are observed in the dihedral angles. Chair conformations were predicted by functional hybrid B3LYP/6-31G* calculations for the rings D and E, as was reported by Karle [21].

Analyzing the distances, it is very important to observe that the bond length C7-C12 in morphine is shorter than the naloxone species while, on the contrary, the bond lengths C17=O3 are longer in the species of morphine because these distances in the naloxone species present double bonds characters. Some differences in the ring E of naloxone species are observed in relation to the morphine ones, thus, on the N atom the CH_3 group present in morphine is replaced by allyl chain in the naloxone

species. In relation to the C-N distances, in the three species of naloxone are observed different values among them and different from the morphine species. As in similar cationic alkaloids species, the N atom in this species of naloxone is positively charged while in the hydrochloride species there is clearly an ionic N-H$^+$Cl- bond between the NH group and the Cl$^-$ anion.

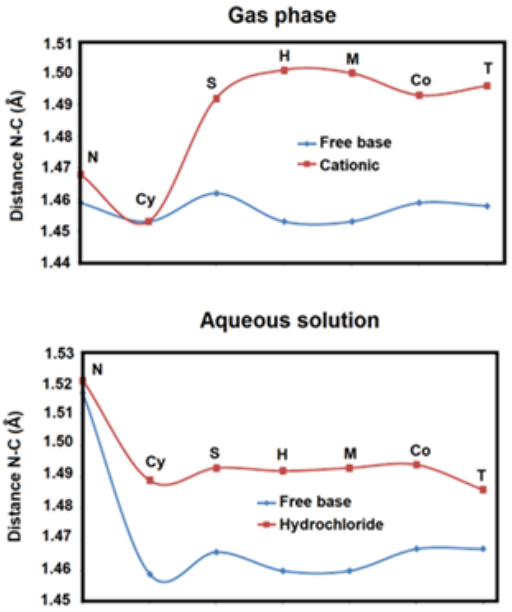

Figure 3. Variations distances N-C of three species of naloxone (N) by using the B3LYP/6-31G* method compared with the corresponding to, Cyclizine (Cy) [17], Morphine (M) [1], Cocaine (Co) [3], Scopolamine (S) [7], Heroin (H) [5] and Tropane (T) [2].

In **Table 4** are presented the C-N distances for the three species of naloxone compared with species containing >N-CH$_3$ bonds while in **Figure 3** are graphed the differences among them. Note that few variations in the N-C bonds are observed in all free base species in gas phase while the distances of all cationic species increase notably in this medium, with exception of cyclizine and naloxone species. The situation change in solution because the free base and hydrochloride species of naloxone present the higher values probably due to the repulsion of charges between the N and Cl atoms and to the allyl chain different from the other species where the N atoms are linked to CH$_3$ groups.

Charges, molecular electrostatic potential and bond orders studies.

Atomic charges, molecular electrostatic potentials and bond orders are important factors that explain the behaviours of different species in different medium. These parameters are of interest in the naloxone species due to that the N5-C19-C23=C24 allyl chain, different from the tropane alkaloids, confer to these species interesting properties in both media. Hence, atomic Mulliken, Merz-Kollman (MK), NPA charges and bond orders on the O atoms and on the N and C atoms belonging to the allyl chain were studied for the three species of naloxone in both media by using the 6-31G* level of theory. Then, in **Table 5** can be seen the results of those three charges for the three species of naloxone in both media by using B3LYP/6-31G* method together with the corresponding values of molecular electrostatic potentials (MEP) and bond orders (BO), expressed as Wiberg indexes. According to the atoms labelling, the C19, C23 and C24 atoms correspond to number's atoms (6), (7) and (8), respectively. On the other hand, the variations of different charges for the three species of naloxone in both media are represented in **Figure 4**.

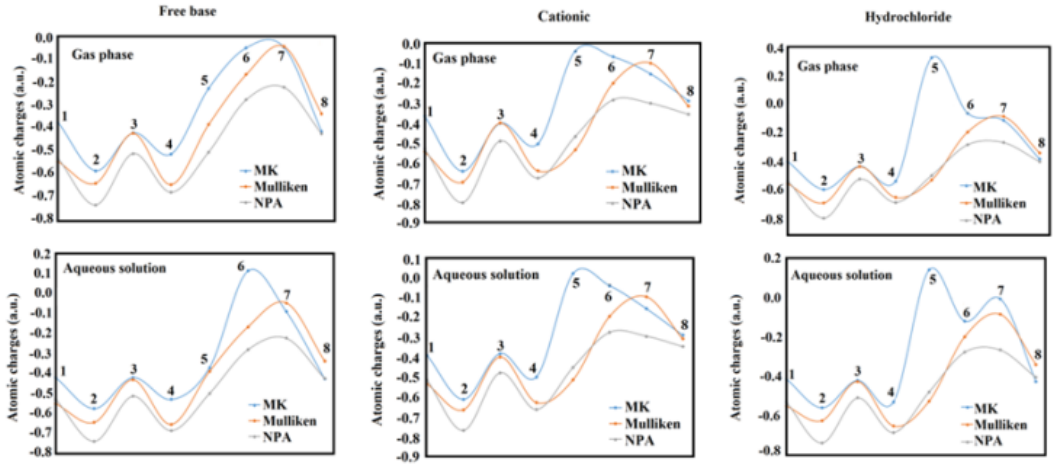

Figure 4. Calculated MK, Mulliken and NPA charges on the O1, O2, O3, O4, N5, C19, C23 and C24 atoms corresponding to the free base, cationic and hydrocloride species of naloxone in both media by using the B3LYP/6-31G* method.

Table 3. Comparison of calculated geometrical parameters for the free base, cationic and hydrochloride naloxone species in gas and aqueous solution phases compared with the corresponding experimental ones for free base and hydrochloride species of morphine.

Parameters	B3LYP/6-31G*[a]						Exp[b]	Exp[c]
	Free base		Cationic		Hydrochloride			
	Gas	PCM	Gas	PCM	Gas	PCM		
Bond lengths (Å)								
N5-C19	1.459	1.468	1.523	1.517	1.513	1.521	1.490	1.492(2)
N5-C8	1.469	1.483	1.540	1.532	1.533	1.540	1.530	1.517(2)

Parameters	B3LYP/6-31G*[a]						Exp[b]	Exp[c]
	Free base		Cationic		Hydrochloride			
	Gas	PCM	Gas	PCM	Gas	PCM		
N5-C14	1.462	1.470	1.517	1.511	1.506	1.509	1.510	1.497(2)
C7-C6	1.550	1.549	1.550	1.549	1.551	1.549	1.550	1.538 (2)
C7-C8	1.562	1.563	1.559	1.558	1.572	1.560	1.550	1.575 (2)
C6-C10	1.547	1.546	1.550	1.549	1.546	1.547	1.540	1.543(2)
C10-C14	1.532	1.531	1.528	1.527	1.525	1.524	1.520	1.516 (2)
C6-C11	1.510	1.510	1.510	1.509	1.508	1.508	1.500	1.503 (2)
C8-C13	1.566	1.563	1.544	1.544	1.552	1.547	1.540	1.540 (2)
C11=C15	1.383	1.383	1.383	1.382	1.384	1.382	1.360	1.380 (2)
C13-C15	1.516	1.515	1.517	1.515	1.518	1.515	1.520	1.511 (2)
C11-C18	1.382	1.384	1.382	1.383	1.381	1.383	1.370	1.370 (2)
C6-C9	1.558	1.554	1.560	1.554	1.553	1.554	1.550	1.549 (2)
C9-O1	1.454	1.463	1.446	1.460	1.461	1.461	1.470	1.466 (18)
C18-O1	1.384	1.391	1.382	1.389	1.379	1.390	1.370	1.377 (17)
C9-C17	1.549	1.542	1.551	1.543	1.551	1.543	1.520	1.536 (2)
C7-C12	1.539	1.539	1.534	1.534	1.543	1.537	1.360	1.320 (2)
C16-C12	1.545	1.545	1.545	1.543	1.543	1.543	1.490	1.506 (2)
C17=O3	1.211	1.222	1.207	1.221	1.212	1.221	1.460	1.419 (19)
C21-O4	1.365	1.378	1.353	1.375	1.361	1.375	1.370	1.375 (2)
C7-O2	1.432	1.437	1.441	1.439	1.409	1.429		
RMSD[b]	**0.073**	**0.070**	**0.071**	**0.068**	**0.071**	**0.069**		
RMSD[c]	**0.070**	**0.068**	**0.069**	**0.067**	**0.069**	**0.067**		
Bond angles (º)								
C19-N5-C8	114.6	112.6	114.1	113.6	113.0	111.8	111.0	112.9(14)
C19-N5-C14	113.3	111.5	112.5	112.4	112.1	111.6		111.8(13)
C8-N5-C14	115.1	113.9	112.9	113.3	114.5	113.4	114.0	112.69(13)
N5-C14-C10	111.3	112.0	110.9	111.2	111.1	112.1	109.0	111.09(13)
N5-C8-C7	108.1	108.8	104.9	105.4	109.5	107.8		106.60(12)
C8-C7-C6	105.3	105.4	106.3	106.1	105.0	106.1		107.56(12)
C14-C10-C6	110.9	111.0	111.3	111.7	111.2	111.7		112.00(13)
C7-C6-C10	108.2	108.5	108.9	109.1	108.7	108.7	111.0	109.10(12)
C7-C6-C11	108.5	108.6	108.4	108.6	108.9	108.7	112.0	106.19(12)
C6-C11-C15	128.0	127.5	128.1	127.6	128.0	127.4	112.0	126.61(14)
C8-C13-C15	113.8	114.1	113.9	114.2	113.6	114.2		114.53(14)
C11-C15-C13	117.3	117.4	117.6	117.8	117.3	117.7	123.0	118.42(14)
C9-C6-C11	97.5	97.7	97.9	98.2	98.1	98.1	109.0	100.58(12)
C9-O1-C18	104.2	104.3	104.8	104.6	104.5	104.6		106.96(11)
C7-C6-C9	118.6	118.3	118.5	117.9	117.9	118.1	111.0	115.78(12)
C6-C9-C17	113.3	113.3	112.7	113.5	113.6	113.4	111.0	112.69(12)
RMSD[b]	**7.2**	**7.0**	**7.1**	**6.8**	**7.0**	**6.8**		
RMSD[c]	**1.8**	**1.6**	**1.5**	**1.3**	**1.7**	**1.4**		
Dihedral angles (º)								
C10-C14-N5-C19	-172.4	-178.5	-173.7	-175.4	-179.7	178.1		
C7-C8-N5-C19	165.3	171.6	166.4	167.3	174.1	174.4		
N5-C8-C7-C6	64.3	64.2	67.1	66.8	61.7	64.4		
N5-C8-C13-C15	-83.9	-83.5	-86.7	-87.1	-82.3	-83.8		
C8-C7-C6-C9	165.8	166.3	164.0	164.8	165.3	165.2		

Parameters	B3LYP/6-31G*[a]						Exp[b]	Exp[c]
	Free base		Cationic		Hydrochloride			
	Gas	PCM	Gas	PCM	Gas	PCM		
C8-C7-C6-C11	55.8	56.1	53.6	54.3	54.7	54.7		
C8-C7-C12-C16	-173.7	-174.2	-173.8	-174.6	-175.6	-174.8		
C13-C15-C11-C18	-171.2	-170.9	-171.4	-171.7	-169.2	-170.1		
O1-C18-C21-O4	2.6	3.1	1.7	2.3	2.9	2.8		
O3-C17-C9-O1	-27.9	-28.1	-24.5	-27.8	-29.8	-28.4		
O3-C17-C16-C12	129.2	129.4	124.6	128.7	129.3	129.4		

[a]This work, [b]Ref [46,47] for hydrochloride morphine; [c]Ref [48] for free base morphine. Bold letters: comparisons expressed as RMSD

Table 4. Bond lengths observed between the N and C atoms belonging to the three naloxone species in gas phase and in aqueous solution by using B3LYP/6-31G* calculations.

N-C-C=C bond						
Species	Gas phase			Aqueous solution		
	Free base	Cationic	Hydrobromide	Free base	Cationic	Hydrobromide
Naloxone[a]	1.459	1.468	1.523	1.517	1.513	1.521
N-CH_3 bond						
Cyclizine[b]	1.453	1.453	[#]	1.459	[#]	1.489
Scopolamine[c]	1.462	1.492	1.491	1.466	1.491	1.493
Heroin[d]	1.453	1.501	1.483	1.460	1.498	1.492
Morphine[e]	1.453	1.500	1.483	1.460	1.497	1.493
Cocaine[f]	1.459	1.493	1.487	1.467	1.492	1.494
Tropane[g]	1.458	1.496	1.478	1.467	1.491	1.486

[#]Imaginary frequencies, [a]This work, [b]Ref [17], [c]From Ref [7], [d]From Ref [5], [e]From Ref [1], [f]From Ref [3], [g]From Ref [2]

On the other hand, the predicted dihedral N5-C19-C23=C24 angles values for the free base, cationic and hydrochloride species of naloxone in gas phase and aqueous solution are respectively -128.7 and -127.3 º, -117.8 and -122.6 º and, -125.2 and -123.5 º different from the experimental value reported by Karle of -98 º [21]. Evidently, the calculations performed in gas phase different from in solid state justify such differences.

Table 5. Mulliken, Merz-Kollman and NPA charges (a.u.), molecular electrostatic potentials (MEP) (a.u.) and bond orders, expressed as Wiberg indexes for the three species of naloxone in gas phase and in aqueous solution by using B3LYP/6-31G* calculations.

FREE BASE										
	GAS					PCM				
Atoms	MK	Mulliken	NPA	MEP	BO	MK	Mulliken	NPA	MEP	BO
1 O	-0.377	-0.551	-0.535	-22.278	2.080	-0.423	-0.554	-0.533	-22.278	2.078
2 O	-0.591	-0.647	-0.742	-22.309	1.813	-0.578	-0.647	-0.743	-22.308	1.812
3 O	-0.425	-0.427	-0.515	-22.316	2.062	-0.422	-0.433	-0.516	-22.319	2.055
4 O	-0.518	-0.653	-0.686	-22.284	1.926	-0.532	-0.657	-0.689	-22.284	1.919
5 N	-0.229	-0.388	-0.509	-18.359	3.133	-0.372	-0.391	-0.502	-18.358	3.123
19 C	-0.050	-0.167	-0.278	-14.710	3.876	0.114	-0.168	-0.282	-14.710	3.878
23 C	-0.048	-0.044	-0.224	-14.742	3.959	-0.090	-0.047	-0.224	-14.740	3.958
24 C	-0.419	-0.341	-0.429	-14.748	3.913	-0.428	-0.339	-0.427	-14.746	3.913
CATIONIC										
1 O	-0.358	-0.535	-0.521	-22.167	2.095	-0.392	-0.538	-0.518	-22.166	2.093
2 O	-0.630	-0.684	-0.786	-22.151	1.783	-0.618	-0.670	-0.775	-22.149	1.795
3 O	-0.394	-0.393	-0.482	-22.211	2.092	-0.385	-0.402	-0.483	-22.215	2.082
4 O	-0.496	-0.628	-0.665	-22.184	1.960	-0.503	-0.634	-0.669	-22.185	1.948
5 N	-0.037	-0.524	-0.459	-18.084	3.459	0.021	-0.518	-0.456	-18.080	3.461
19 C	-0.066	-0.196	-0.279	-14.530	3.802	-0.040	-0.196	-0.278	-14.528	3.800
23 C	-0.150	-0.096	-0.296	-14.589	3.943	-0.156	-0.096	-0.297	-14.587	3.944
24 C	-0.283	-0.308	-0.350	-14.601	3.890	-0.292	-0.310	-0.350	-14.599	3.889
HYDROCHLORIDE										
1 O	-0.397	-0.550	-0.532	-22.267	2.087	-0.410	-0.548	-0.527	-22.252	2.086
2 O	-0.591	-0.685	-0.791	-22.319	1.779	-0.557	-0.622	-0.735	-22.279	1.826
3 O	-0.429	-0.431	-0.519	-22.317	2.060	-0.418	-0.424	-0.507	-22.298	2.063
4 O	-0.532	-0.647	-0.681	-22.270	1.934	-0.528	-0.649	-0.682	-22.260	1.930

5 N	0.330	-0.524	-0.493	-18.232	3.387	0.142	-0.524	-0.477	-18.221	3.408
19 C	-0.057	-0.188	-0.278	-14.653	3.825	-0.117	-0.197	-0.275	-14.659	3.819
23 C	-0.108	-0.080	-0.263	-14.711	3.933	-0.004	-0.083	-0.264	-14.726	3.921
24 C	-0.378	-0.334	-0.396	-14.716	3.908	-0.424	-0.338	-0.403	-14.726	3.910

Analyses of different curves presented in figure clearly show that the behaviours of Mulliken and NPA charges on those eight atoms of three species of naloxone in both media are approximately the same while important differences in the behaviours of MK charges on the N5, C19, C23 and C24 atoms are observed. Hence, the three charge's types evidence that the O1 and O3 atoms, corresponding to B rings and to C17=O3 groups of three species present the less negative and different values and they are strongly depending on medium. Thus, the MK charges on O1 and O3 atoms in the free base species in both media have practically the same values while the two other charges on O3 atoms are slightly higher than the observed on the O1 atoms. On the contrary, in the cationic and hydrochloride species are observed important variations in the three charges on the N5, C19, C23 and C24 atoms. The MK and Mulliken charges on the C19 (Nº 6) and C23 (Nº 7) atoms of free base species present practically the same values in gas phase, however, in aqueous solution the MK charges on C19 increase notably in relation to the observed on C23. Different situations are observed in the cationic and hydrochloride species. In the cationic species, the MK charges on N5 atoms in both media present higher values than the other ones while in the hydrochloride ones the charges on C19 atoms are notably lower than the N5 and C23 atoms. In the latter species, the presence of Cl47 atom linked to N5-H47 bond clearly modifies the MK charges on allyl group. Obviously, these studies show that the MK charges explain better the behaviours of three species in the two media and that only the MK charges on the N5 atoms in the hydrochloride species in both media present positive signs while in the cationic species only in solution that atom shows positive sign. These results are important because confirm the ionic characteristics of N-H···Cl bonds in the hydrochloride species, as we will see later in the NBO and AIM studies.

If now the molecular electrostatic potentials (MEP) are analyzed from Table 5 few differences among the values for the three different species are observed due to the proximities of their values. However, when the mapped surfaces are generated with the *GaussView* program [41], the different colorations evidence clearly different regions or sites of reactivity, as shown in **Figure 5**. Thus, strong red colours are observed on the nucleophilic sites, N5 and O3 atoms (C=O) while on the H atoms of both OH groups are observed blue colours due to that these atoms are electrophilic sites. The cationic species is strongly electrophilic because it is a positively charged species while in the hydrochloride species the strong nucleophilic region is located on the Cl atom, as expected due to its high electronegativity value. Besides, Figure 5 shows that allyl chain in the free base presents green coloration while in the hydrochloride species change to light blue colour, revealing that the nature of charges on allyl group change in that species, as evidenced by MK charges on the allyl N5-C19-C23=C24 chain. From this study, it is possible to predict the different sites where reactions with nucleophilic and/or electrophilic reactive can occur.

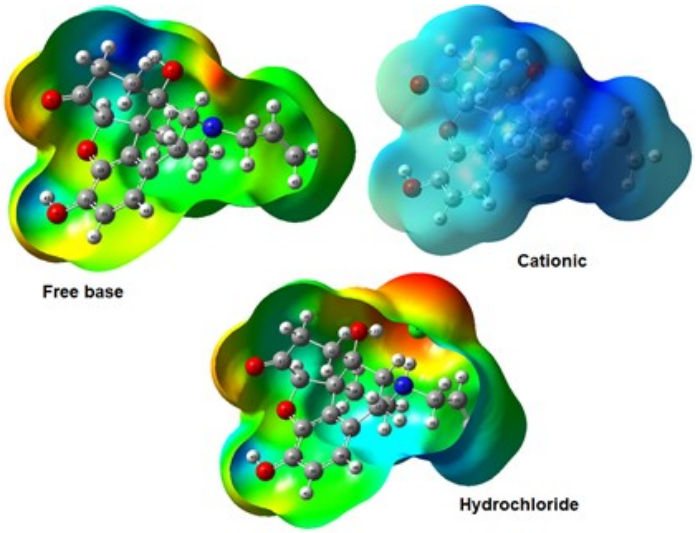

Figure 5. Calculated electrostatic potential surfaces on the molecular surfaces of the free base (0.0615 a.u.), cationic and hydrochloride (0.0647 a.u.) species of naloxone in gas phase. B3LYP functional and 6-31G* basis set. Isodensity value of 0.005.

For the three naloxone species in both media were also analyzed the bond orders (BO), expressed as Wiberg indexes, by using the 6-31G* level of theory. The values presented in Table 5 are those totals by atoms obtained with the NBO program [44] only for the allyl chain. For the three species of naloxone in both media are not observed significant changes in the values and, only, the O2 atoms present the lower values while the higher ones are observed for the C23 atoms. The N5 and C23 atoms corresponding to the cationic species in both media have the higher BO values while the C24 atoms corresponding to the free base in the two media present the higher values than the other ones. On the other hand, the high BO values obtained with the corresponding Wiberg bond index matrix in the Natural Atomic Orbital (NAO) basis for the O3, C17, C23 and C24 atoms in the three species reveal the double bonds characters of both C23=C24 and C17=O3 bonds.

Stabilities studies based on NBO and AIM analyses

The above studies have evidenced the influence of atomic MK charges on the four involved atoms of allyl N5-C19-C23=C24 chain in the three species of naloxone supporting different colorations on their mapped surfaces. On the other hand, the studies of donor-acceptor energies and inter or intra-molecular interactions and topological properties of free base, cationic and hydrochloride species of naloxone are of great interest to know the role of allyl chain and of the five different rings in the stabilities of these narcotic agents [44,45]. Therefore, the second order perturbation theory analyses of Fock matrix in NBO Basis were first computed for the three species by using the NBO program [44]. Hence, in **Table 6** are summarized the main delocalization energies for three species of naloxone in both media by using the B3LYP/6-31G* method. Analyzing the results it is observed commons $\Delta E_{\pi\rightarrow\pi^*}$, $\Delta E_{LP\rightarrow\pi^*}$ and $\Delta E_{LP\rightarrow\sigma^*}$ interactions in the three species in the two media while only for the free base in both media are observed the $\pi^*C18\text{-}C21\rightarrow \pi^*C11\text{-}C15$ and $\pi^*C20\text{-}$

*C22→π*C11-C15* interactions and only for the hydrochloride species the $\Delta E_{\sigma^*\to LP^*}$, *LP(3)Cl47→σ*O2-H37, LP(4)Cl47→σ*O2-H37, LP(4)Cl47→σ*N5-H46* and $\Delta E_{LP\to LP^*}$ interactions are observed. In the $\Delta E_{\pi\to\pi^*}$ interactions are implicated transitions from π bonding C=C orbitals to π anti-bonding C=C orbitals of D rings of the three species while in $\Delta E_{LP\to\pi^*}$ and $\Delta E_{LP\to\sigma^*}$ are involved transitions from lone pairs of O1, O3, O4, N5 and Cl47 atoms to π C=C orbitals and to σ anti-bonding C9-C17, C16-C17, O2-H37 and N5-H46 orbitals, as detailed in Table 6. Here, these transitions show clearly that the A and B rings also participle in the interactions. The evaluation of the $\Delta E_{\sigma^*\to LP^*}$ and $\Delta E_{LP\to LP^*}$ interactions in the hydrochloride species in gas phase shows that in these interactions are involved transitions from σ bonding N-C orbitals and lone pairs of N5 and Cl47 atoms toward lone pairs antibonding of H46 atom. Thus, the E ring and the allyl chain participle only in the hydrochloride species in gas phase while in solution in this species disappear the *LP(3)Cl47→σ*O2-H37* and *LP(4)Cl47→σ*O2-H37* interactions but appear the *LP(4)Cl47→σ*N5-H46* interaction. The estimation of total energy for each species clearly shows that the free base is the most stable species in both media with ΔE_{TOTAL} values in gas phase and in solution of 3158.87 and 3127.56 kJ/mol, respectively. These results are in agreement with the low solvation energy value in aqueous solution indicating that it is the less soluble species. Later, the hydrochloride species in gas phase, with a value of 3060.35 kJ/mol, is most stable than the corresponding in solution (952.91 kJ/mol). Here, the cationic species is visibly the less stable species in both media because it exists in aqueous solution and has the most negative solvation energy value (-302.45 kJ/mol), similar to morphine alkaloid. The high stabilities of free base in both media are obviously supported by the transitions related to D rings while the high stability of hydrochloride species in gas phase is associated with the participation of other A, B and E rings and to N-C bond of allyl chain. In solution, transitions related to E ring and to the *LP(3)Cl47→σ*O2-H37* and *LP(4)Cl47→σ*O2-H37* interactions are not observed in the hydrochloride species while the *LP(4)Cl47→σ*N5-H46* interaction is observed because it species is as cationic one in solution.

NBO studies have evidenced the participation of four of five rings and of N-C bond of allyl chain in the three naloxone species, with exception of C ring. Now, inter or intra-molecular interactions of free base, cationic and hydrochloride species of naloxone are investigated in both media by means of the topological properties. In this case, the Bader's theory is useful to explore those properties with the AIM2000 program [45,49]. Thus, the electron density, $\rho(r)$, the Laplacian values, $\nabla^2\rho(r)$, the eigenvalues $(\lambda 1, \lambda 2, \lambda 3)$ of the Hessian matrix and, the $|\lambda 1|/\lambda 3$ ratio have been calculated in the bond critical points (BCPs) and ring critical points (RCPs) for all species in both media with the B3LYP/6-31G* method. The results of these properties by using the B3LYP/6-31G* method for free base and cationic species in both media can be seen in **Table 7** while for the hydrochloride species in the two media are observed in **Table 8**. Here, it is necessary to remember that an interaction is ionic or highly polar covalent when $\lambda 1/\lambda 3 < 1$ and $\nabla^2\rho(r) > 0$ (closed-shell interaction). New H bonds interactions generate in the three species in both media are detailed in Tables 7 and 8 and the same are clearly shown in the corresponding molecular graphics of each species in gas phase in **Figure 6**.

In the free base in gas phase is observed the C16-H35···H37 interaction which generates the new RCPN while in solution disappear this interaction probably because the distance between both atoms increases in this medium from 2.005 Å in gas phase to 2.112 Å in solution. The exhaustive analyses of RCPs corresponding to A, B, C, D and E rings evidence that the properties of A and B rings have changed when the medium change from gas phase to solution while the properties for the other ones remain practically constant.

Besides, the higher values of $\rho(r)$ and $\nabla^2\rho(r)$ are observed for the B ring of free base in both media and, then, for the D ring. In the cationic species in both media are predicted the H bonds C7-O2···H46 interactions, different from the free base, where clearly the properties of B ring and of these new interactions are higher than the other ones. In the hydrochloride species in gas phase are observed five different H bonds interactions which can be easily seen in Figure 6. The topological properties of those five interactions are different among them evidencing that they present different characteristics (C13-H32···H38, C23-H42···Cl47, C10-H27···Cl47, N5-H46···Cl47 and O2-H37···Cl47 interactions). These five interactions generate four new RCPs named RCPN1, RCPN2, RCPN3, and RCPN4 which correspond respectively to C10-H27···Cl47, O2-H37···Cl47, C23-H42···Cl47, N5-H46···Cl47 and C13-H32···H38. Here, the two C23-H42···Cl47 and N5-H46···Cl47 interactions generate one only RCPN3. In solution, the number of interactions is reduced to three with the formation of only two RCPs, RCPN3 and RCPN4.

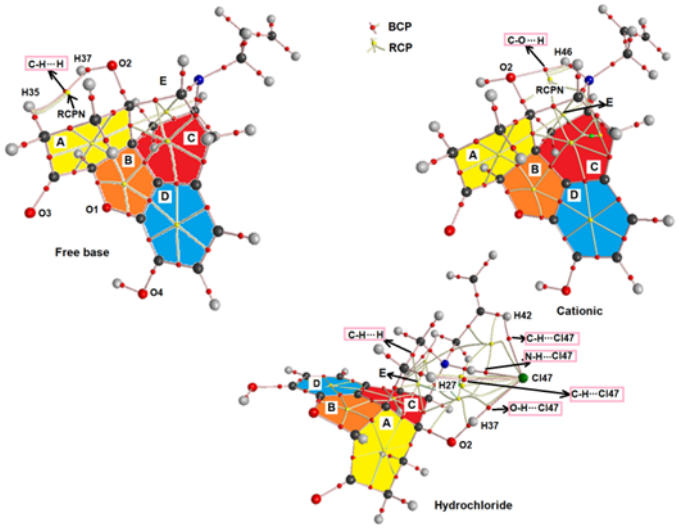

Figure 6. Molecular graphics of three species of naloxone in gas phase showing their H bonds interactions by using the B3LYP/6-31G* method. Rings A, B, C, D and E are identified by different colorations.

In both media, the N5-H46···Cl47 interactions present the higher topological properties, as expected because the N5 atom is positively charged while the Cl47 atom is negatively charged being ionic this interaction. Hence, the hydrochloride species is as cationic one, especially in aqueous solution. According to IUPAC the representation of this interaction should be $H46^{+}Cl47^{-}$. The Wiberg bond index matrix in the NAO basis for the H46 atom in gas phase is 0.5255 while the Cl47 atom is 0.0675. In solution, the value for the H46 atom slightly increases to 0.5805 while

decreases to 0.0378 for the Cl47 atom, showing this way that the N5-H46···Cl47 bonds have ionic characteristics in both media. These NBO and AIM studies support clearly that the hydrochloride species is as cationic one in both media.

Frontier orbitals and quantum global descriptors studies.

Reactivities of different species are predicted by using the gap values calculated from the molecular frontier orbitals, as suggested by Paar and Pearson [31] while the predictions of its behaviours are performed with some important descriptors by using equations recommended in the literature [32-40]. Here, the HOMO, LUMO and energy band gaps for the three species of naloxone in both media were calculated with the B3LYP/6-31G* method and the results are presented in **Table 9**. In the same Table are summarized the chemical potential (μ), electronegativity (χ), global hardness (η), global softness (S), global electrophilicity index (ω) and global nucleophilicity index (E) descriptors [32-40]. Note that the equations used to calculate the descriptors are also presented in that table. Comparisons of gap values of these species with values reported for S(-)-Promethazine [8], R(+)-Promethaine [8], Cyclizine (Cy) [17], Morphine (M) [1], Cocaine (Co) [3], Scopolamine (S) [7], Heroin (H) [5] and Tropane (T) [2] can be seen in **Table 10** while in **Figure 7** are observed their behaviours in both media. Here, it is necessary to clarify that I letters indicated in Table 10 for cationic S(-) form of promethazine and cyclizine in solution and for the hydrochloride species of cyclizine in gas phase represent optimized calculations with imaginary frequencies and, for these reasons, their corresponding values are not presented. Analyzing the gap values for the three species of naloxone we observed that the hydrochloride species in solution presents the lowest value (2.9686 eV) showing its higher reactivity in solution, because this species in this medium is as cationic one while in gas phase it is less reactive due to its higher gap value. On the contrary, the cationic species in both media evidence lower reactivity than the free base, a result different from expected because its species is positively charged in solution and because from the NBO analysis is the less stable species. These different results probably could be explained from the AIM analysis because the C7-O2···H46 interactions observed for the cationic species in both media show higher values in their topological properties, as compared with the H bond observed for the free base in gas phase while these latter species don't have interaction in solution.

Table 6. Main delocalization energies (in kJ/mol) for the three species of naloxone in gas and aqueous solution phases by using B3LYP/6-31G* calculations.

B3LYP/6-31G*[a]						
Delocalization	Free base		Cationic		Hydrochloride	
	Gas	PCM	Gas	PCM	Gas	PCM
$\pi C11\text{-}C15 \rightarrow \pi^*C18\text{-}C21$	85.48	84.85	76.03	75.74	81.01	80.21
$\pi C11\text{-}C15 \rightarrow \pi^*C20\text{-}C22$	79.38	78.63	72.57	71.85	78.29	76.24
$\pi C18\text{-}C21 \rightarrow \pi^*C11\text{-}C15$	89.66	88.7	97.94	96.35	94.38	92.59
$\pi C18\text{-}C21 \rightarrow \pi^*C20\text{-}C22$	78.75	79.13	75.16	76.03	79.34	78.29
$\pi C20\text{-}C22 \rightarrow \pi^*C11\text{-}C15$	74.74	75.37	79.84	80.76	74.86	76.79
$\pi C20\text{-}C22 \rightarrow \pi^*C18\text{-}C21$	78.12	77.75	79.30	79.42	77.58	77.92
$\Delta E_{\pi \rightarrow \pi^*}$	486.13	484.42	480.83	480.16	485.47	482.04
$\sigma N5\text{-}C8 \rightarrow LP^*H46$					58.85	
$\sigma N5\text{-}C14 \rightarrow LP^*H46$					66.34	
$\sigma N5\text{-}C19 \rightarrow LP^*H46$					65.38	
$\Delta E_{\sigma^* \rightarrow LP^*}$					190.57	
$LP(2)O1 \rightarrow \pi^*C18\text{-}C21$	93.38	93.63	93.84	93.97	97.73	94.97
$LP(2)O4 \rightarrow \pi^*C18\text{-}C21$	114.7	111.4	129.66	121.26	117.54	115.24
$\Delta E_{LP \rightarrow \pi^*}$	208.08	205.03	223.50	215.23	215.27	210.21
$LP(2)O3 \rightarrow \sigma^*C9\text{-}C17$	100.11	95.93	105.71	100.49	102.28	97.77
$LP(2)O3 \rightarrow \sigma^*C16\text{-}C17$	84.73	79.04	88.11	80.09	81.8	79.42
$LP(3)Cl47 \rightarrow \sigma^*O2\text{-}H37$					61.36	
$LP(4)Cl47 \rightarrow \sigma^*O2\text{-}H37$					45.81	
$LP(4)Cl47 \rightarrow \sigma^*N5\text{-}H46$						83.47
$\Delta E_{LP \rightarrow \sigma^*}$	184.84	174.97	193.83	180.58	291.26	260.66
$LP(1)N5 \rightarrow LP^*H46$					1474.95	
$LP(4)Cl47 \rightarrow LP^*H46$					402.83	
$\Delta E_{LP \rightarrow LP^*}$					1877.78	
$\pi^*C18\text{-}C21 \rightarrow \pi^*C11\text{-}C15$	1020.21	997.68				
$\pi^*C20\text{-}C22 \rightarrow \pi^*C11\text{-}C15$	1259.6	1265.45				
$\Delta E_{\pi^* \rightarrow \pi^*}$	2279.81	2263.14				
ΔE_{TOTAL}	3158.87	3127.56	898.16	875.96	3060.35	952.91

[a]This work

Table 7. Analysis of the Bond Critical Points (BCPs) and Ring critical point (RCPs) for the free base and cationic species of naloxone in gas and aqueous solution phases by using the B3LYP/6-31G* method.

B3LYP/6-31G* Method							
FREE BASE							
GAS PHASE							
Parameter[#]	H35-H37	RCPN	RCPA	RCPB	RCPC	RCPD	RCPE
ρ(r)	0.0118	0.0118	0.0163	0.0440	0.0185	0.0204	0.0181
$\nabla^2\rho(r)$	0.0513	0.0528	0.1014	0.3084	0.1183	0.1604	0.1176
λ1	-0.0118	-0.0111	-0.0124	-0.0443	-0.0135	-0.0148	-0.0128
λ2	-0.0016	0.0017	0.0524	0.1559	0.0505	0.0731	0.0617
λ3	0.0647	0.0622	0.0614	0.1967	0.0812	0.1021	0.0687
|λ1|/λ3	0.1824	0.1785	0.2020	0.2252	0.1663	0.1450	0.1863
Distances	2.005						
AQUEOUS SOLUTION							
Parameter[#]			RCPA	RCPB	RCPC	RCPD	RCPE
ρ(r)			0.0166	0.0435	0.0185	0.0204	0.0179
$\nabla^2\rho(r)$			0.1036	0.3051	0.1187	0.1598	0.1155
λ1			-0.0127	-0.0437	-0.0134	-0.0148	-0.0130
λ2			0.0541	0.1553	0.0517	0.0728	0.0597
λ3			0.0621	0.1934	0.0804	0.1018	0.0687
|λ1|/λ3			0.2045	0.2260	0.1667	0.1454	0.1892
CATIONIC							
GAS PHASE							
Parameter[#]	O2-H46	RCPN	RCPA	RCPB	RCPC	RCPD	RCPE
ρ(r)	0.0266	0.0224	0.0163	0.0439	0.0186	0.0203	0.0178
$\nabla^2\rho(r)$	0.1039	0.1380	0.1015	0.3097	0.1186	0.1598	0.1108
λ1	-0.0320	-0.0196	-0.0123	-0.0442	-0.0138	-0.0148	-0.0130
λ2	-0.0264	0.0369	0.0526	0.1595	0.0489	0.0725	0.0614
λ3	0.1624	0.1207	0.0612	0.1944	0.0835	0.1021	0.0624
|λ1|/λ3	0.1970	0.1624	0.2010	0.2274	0.1653	0.1450	0.2083
Distances	1.982						
AQUEOUS SOLUTION							
Parameter[#]	O2-H46	RCPN	RCPA	RCPB	RCPC	RCPD	RCPE
ρ(r)	0.0248	0.0218	0.0165	0.0434	0.0186	0.0204	0.0179
$\nabla^2\rho(r)$	0.0905	0.1253	0.1034	0.3052	0.1191	0.1600	0.1118
λ1	-0.0298	-0.0200	-0.0125	-0.0437	-0.0139	-0.0148	-0.0130
λ2	-0.0223	0.0315	0.0547	0.1572	0.0501	0.0729	0.0616
λ3	0.1426	0.1137	0.0612	0.1917	0.0828	0.1019	0.0631
|λ1|/λ3	0.2090	0.1759	0.2042	0.2280	0.1679	0.1452	0.2060
Distances	2.058						

[#]Parameters in a.u., Distances in Å

Table 8. Analysis of the Bond Critical Points (BCPs) and Ring critical point (RCPs) for the hydrochloride species of naloxone in gas and aqueous solution phases by using the B3LYP/6-31G* method.

B3LYP/6-31G* Method					
HYDROCHLORIDE					
GAS PHASE					
Parameter[#]	Cl47-H27	Cl47-H37	Cl47-H42	Cl47-H46	H32-H38
ρ(r)	0.0059	0.0327	0.0095	0.0556	0.0120
$\nabla^2\rho(r)$	0.0188	0.0828	0.0324	0.0996	0.0495
λ1	-0.0016	-0.0409	-0.0077	-0.0800	-0.0116
λ2	-0.0016	-0.0389	-0.0057	-0.0790	-0.0063
λ3	0.0221	0.1626	0.0458	0.2586	0.0674
|λ1|/λ3	0.0724	0.2515	0.1681	0.3094	0.1721
Distances	3.121	2.098	2.777	1.884	2.058
Parameter[#]	RCPN1	RCPN2	RCPN3		RCPN4

ρ(r)	0.0058	0.0105	0.0079		0.0115
$\nabla^2\rho(r)$	0.0202	0.0524	0.0323		0.0552
λ1	-0.0017	-0.0085	-0.0056		-0.0086
λ2	0.0020	0.0107	0.0079		0.0078
λ3	0.0198	0.0501	0.0299		0.0559
|λ1|/λ3	0.0859	0.1697	0.1873		0.1538
Ring critical points					
Parameter[#]	RCPA	RCPB	RCPC	RCPD	RCPE
ρ(r)	0.0163	0.0439	0.0186	0.0204	0.0176
$\nabla^2\rho(r)$	0.1026	0.3090	0.1184	0.1602	0.1094
λ1	-0.0128	-0.0444	-0.0136	-0.0148	-0.0127
λ2	0.0535	0.1595	0.0488	0.0730	0.0572
λ3	0.0618	0.1938	0.0832	0.1019	0.0648
|λ1|/λ3	0.2071	0.2291	0.1635	0.1452	0.1960
AQUEOUS SOLUTION					
Parameter[#]	Cl47-H42	Cl47-H46	RCPN3	H32-H38	RCPN4
ρ(r)	0.0123	0.0243	0.0068	0.0138	0.0120
$\nabla^2\rho(r)$	0.0384	0.0529	0.0264	0.0537	0.0601
λ1	-0.0108	-0.0264	-0.0038	-0.0150	-0.0095
λ2	-0.0096	-0.0260	0.0113	-0.0105	0.0130
λ3	0.0587	0.1054	0.0188	0.0793	0.0565
|λ1|/λ3	0.1840	0.2505	0.2021	0.1892	0.1681
Distances	2.650	2.297		1.960	
Parameter[#]	RCPA	RCPB	RCPC	RCPD	RCPE
ρ(r)	0.0165	0.0434	0.0185	0.0204	0.0175
$\nabla^2\rho(r)$	0.1034	0.3056	0.1194	0.1601	0.1091
λ1	-0.0126	-0.0438	-0.0136	-0.0148	-0.0129
λ2	0.0540	0.1573	0.0515	0.0728	0.0582
λ3	0.0619	0.1919	0.0814	0.1021	0.0638
|λ1|/λ3	0.2036	0.2282	0.1671	0.1450	0.2022

[#]Parameters in a.u., Distances in Å

Table 9. Frontier molecular HOMO and LUMO orbitals and gap values (in eV) for the three naloxone species in gas and aqueous solution phases by using the B3LYP/6-31G* level of theory.

B3LYP/6-31G* Method[a]						
Orbital	FREE BASE		CATIONIC		HYDROCHLORIDE	
	Gas	PCM	Gas	PCM	Gas	PCM
HOMO	-5.5280	-5.6202	-8.6362	-8.7088	-6.0730	-4.5610
LUMO	-0.9760	-0.9820	-3.8850	-3.8981	-0.9989	-1.5924
|GAP|	4.552	4.6382	4.7512	4.8107	5.0741	2.9686
DESCRIPTORS						
χ	-2.2760	-2.3191	-2.3756	-2.4054	-2.5371	-1.4843
μ	-3.2520	-3.3011	-6.2606	-6.3035	-3.5360	-3.0767
η	2.2760	2.3191	2.3756	2.4054	2.5371	1.4843
S	0.2197	0.2156	0.2105	0.2079	0.1971	0.3369
ω	2.3233	2.3495	8.2495	8.2594	2.4641	3.1887
E	-7.4016	-7.6556	-14.8727	-15.1620	-8.9709	-4.5667

[a]This work, χ = - [E(LUMO)- E(HOMO)]/2 ; μ = [E(LUMO) + E(HOMO)]/2; η = [E(LUMO) - E(HOMO)]/2; S = ½η; $\omega = \mu^2/2\eta$; E=$\mu*\eta$

If now the gap values are compared for all free base species, it is observed the same behaviours in the two media and, also that the species corresponding to naloxone presents the lower values in both media. For these reasons, the free base of naloxone is the most reactive than the other ones. The cationic species of both forms of promethazine have the lower values and, then, the species of naloxone, hence; the two S and R forms of promethazine have higher reactivities. Apparently, these species show the same behaviours in the two media. In relation to the hydrochloride species, the species of naloxone is the most reactive in solution but in gas phase the cocaine's species evidence a higher reactivity. Note that the three species of tropane in both media are less reactive, as compared with the other ones.

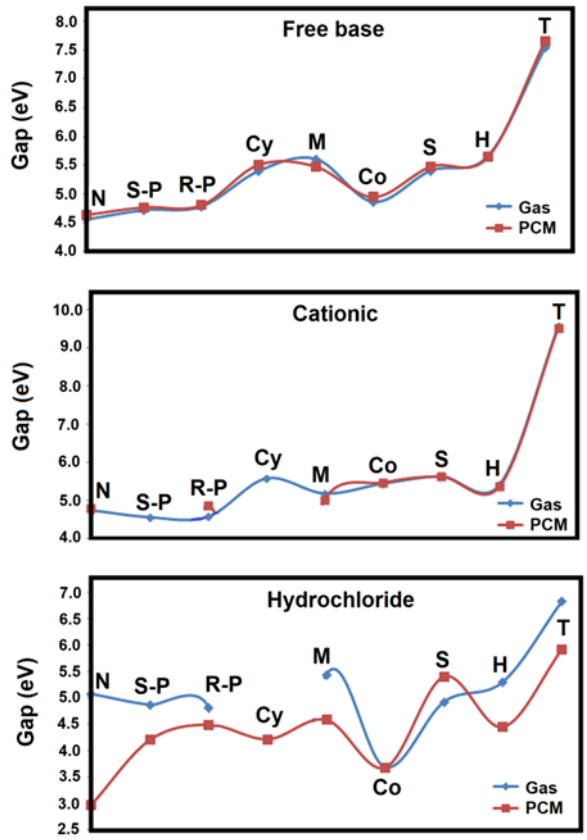

Figure 7. Gap values of three species of naloxone (N) by using the B3LYP/6-31G* method compared with the corresponding to, S(-)-Promethazine (S-P) [8], R(+)-Promethaine (R-P) [8], Cyclizine (Cy) [17], Morphine (M) [1], Cocaine (Co) [3], Scopolamine (S) [7], Heroin (H) [5] and Tropane (T) [2].

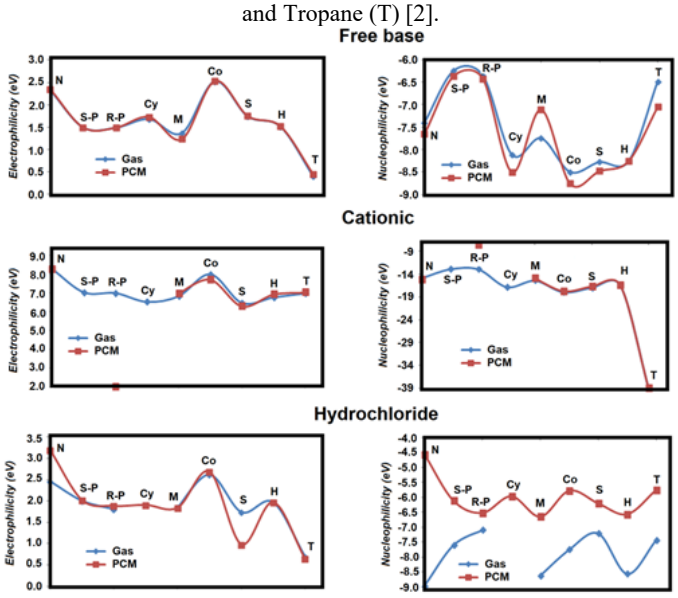

Figure 8. Global electrophilicity (ω) and nucleophilicity (E) indexes for the three species of naloxone compared with other species in gas and aqueous solution phases by using the B3LYP/6-31G* level of theory.

Evidently, the allyl chains present in the three species of naloxone diminishing the gap values increasing their reactivities, as compared with the other ones containing the N-CH_3 group. Hence, the hydrochloride species of naloxone shows the lowest value in solution and, for this reason, is the most reactive species in this medium, as compared with the other ones. Regarding the descriptors from Table 9 it is observed that being the hydrochloride species of naloxone the most reactive in solution it presents lower global hardness (η) and higher global softness (S), than the other ones while, also low global nucleophilicity indexes (E) are observed for that species in both media. In relation to global electrophilicity index (ω), the cationic species of naloxone in the two media show higher values. On the contrary, the free base species of naloxone present the lower values in both media.

In **Table 11**, the global electrophilicity (ω) and global nucleophilicity (E) indexes of three species of naloxone are compared with those reported for S(-)-Promethazine [8], R(+)-Promethaine [8], Cyclizine (Cy) [17], Morphine (M) [1], Cocaine (Co) [3], Scopolamine (S) [7], Heroin (H) [5] and Tropane (T) [2] while in **Figure 8** can be seen the different behaviours of all species.

Table 10. Gap values for the three naloxone species compared with other species in gas phase and aqueous solution by using the B3LYP/6-31G* level of theory.

B3LYP/6-31G* method[a]		
FREE BASE		
Species	Gas	PCM
Naloxone[a]	4.5520	4.6382
S(-)-Promethazine[b]	4.7157	4.7702
R(+)-Promethazine[b]	4.7756	4.8028
Cyclizine[c]	5.3946	5.5067
Morphine[d]	5.6044	5.4750
Cocaine[e]	4.8580	4.9487
Scopolamine[#,f]	5.4004	5.4758
Heroin[g]	5.6563	5.6414
Tropane[f,h]	7.5506	7.6611
CATIONIC		
Naloxone[a]	4.7512	4.8107
S(-)-Promethazine[b]	4.5661	I
R(+)-Promethazine[b]	4.5770	4.8654
Cyclizine[c]	5.5823	I
Morphine[d]	5.1889	5.0244
Cocaine[e]	5.4468	5.4660
Scopolamine[#,f]	5.6356	5.6289
Heroin[g]	5.4268	5.3757
Tropane[f,h]	9.5595	9.5250
HYDROCHLORIDE		
Naloxone[a]	5.0741	2.9686
S(-)-Promethazine[b]	4.8654	4.2042
R(+)-Promethazine[b]	4.8110	4.4926
Cyclizine[c]	I	4.2159
Morphine[d]	5.4417	4.5840
Cocaine[e]	3.6813	3.6813
Scopolamine[#,f]	4.9239	5.4026
Heroin[g]	5.3024	4.4469
Tropane[f,h]	6.8246	5.9119

[#]Hydrobromide, [a]This work, [b]From Ref [8], [c]From Ref [17], [d]From Ref [1], [e]From Ref [3], [f]From Ref [7], [g]From Ref [5], [h]From Ref [2]. I=imaginary frequencies

Analyzing Figure 8, it is easy to observe that the free base of cocaine in both media presents the higher ω values together with the species of naloxone while that species of cocaine also present the most negative E values in both media. Note that the free base species of naloxone shows in both media values near to morphine, probably due to the similarity of their rings.

Evaluating the cationic species we observed that the naloxone species shows the higher values in both media while the lower values are observed in the R(+) form of promethazine and in the scopolamine species. In relation to the *E* values, the most negative values are observed in the tropane species while the less negative values are observed for the R(+) form of promethazine. When the hydrochloride species are compared, it is observed the higher ω values in both media for the species of cocaine and naloxone while the species of scopolamine presents the lower value in solution. This observation could be attributed to Br atom because this species was studied as hydrobromide. When the *E* values are analyzed for the hydrochloride species we observed the less negative values in aqueous solution, as compared with the values in gas phase, because clearly, these species are as cationic ones in this medium. Then, the most negative values are observed for the R(+) form of promethazine, morphine and heroine while that species of naloxone has in solution the less negative value. Hence, this observation could probably be associated with the allyl chain present in the naloxone species.

Vibrational study.

The hybrid B3LYP/6-31G* calculations have optimized the three naloxone species with C_1 symmetries. Comparisons of experimental available ATR and Raman spectra for the hydrochloride species dihydrated of naloxone taken from Ref [30] with those predicted for free base, cationic and hydrochloride forms can be seen in **Figures 9** and **10**, respectively.

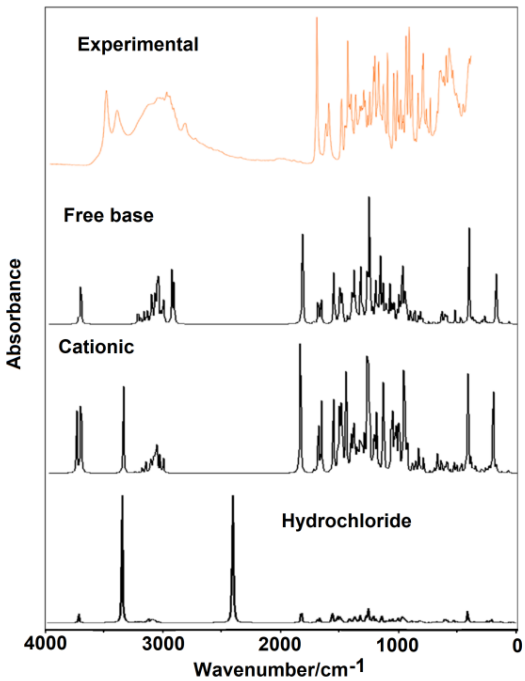

Figure 9. Experimental available ATR spectrum of hydrochloride species dihydrated of naloxone in solid phase [30] compared with the predicted in gas phase for the three species by using the hybrid B3LYP/6-31G* method.

These spectra show good correlations, in particular, the Raman spectra because these predicted spectra in activities were converted to intensities with known equations [50,51]. According to the numbers of atoms present in the structures, for the free base, cationic and hydrochloride species are expected 129, 132 and 135 vibration normal modes, respectively where all they have activities in both spectra. A very important observation is that the strong IR band predicted for the hydrochloride form by using B3LYP/6-31G* calculations at 2405 cm^{-1}, associated with N5-H46 stretching mode, is not observed in the experimental spectrum. Then, its form is not present in the solid phase. The other intense band in the IR spectra of hydrochloride form at 3355 cm^{-1} is assigned to O2-H37 stretching mode, which is also observed for the cationic form at slightly higher wavenumber. In the IR spectrum of free base the band attributed to O2-H37 stretching mode is observed with low intensity and at higher wavenumbers. Here, the scaled quantum mechanical force field (SQMFF) methodology was used together with the normal internal coordinates of each species and the Molvib program in order to perform the complete vibrational assignments of three species [27-29]. The scaling process were employed those scale factors suggested by Rauhut and Pulay [28] while potential energy distribution (PED) contributions ≥ 10 % were used.

In **Table 12** are summarized both, observed and calculated wavenumbers for the three species of naloxone in gas phase together with their corresponding assignments. Obviously, after of apply the SQM procedure the positions of all bands change in relation to those predicted by B3LYP/6-31G* calculations. For instance, the SQM calculations predicted the N5-H46 stretching mode of hydrochloride species at lower wavenumber, which is at 2312 cm^{-1}, as compared with the calculated value and as observed in Table 12. Below, brief discussions of some assignments are presented.

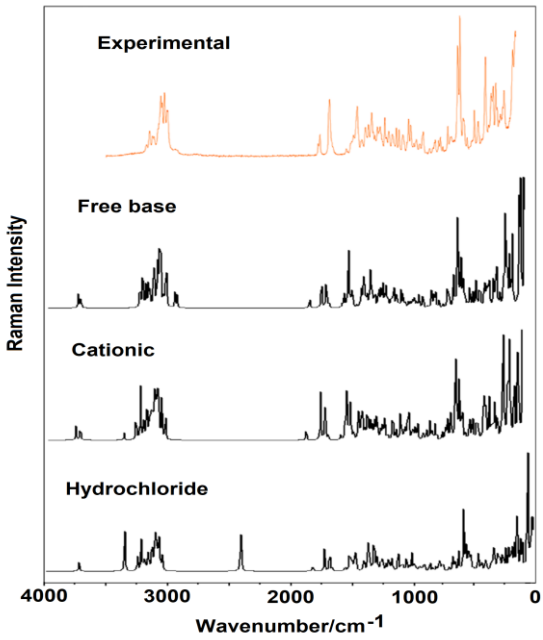

Figure 10. Experimental available Raman spectrum of hydrochloride species dihydrated of naloxone in solid phase [30] compared with the predicted in gas phase for the three species by using the hybrid B3LYP/6-31G* method.

Band Assignments.

NH modes. Vibration modes of N5-H46 groups are expected only for the cationic and hydrochloride species of naloxone. Thus, in the cationic species the SQM/B3LYP/6-31G* calculations have predicted the N5-H46 stretching mode at 3221 cm^{-1} while in the hydrochloride one at 2312 cm^{-1}. In cationic species of cyclizine, scopolamine, heroin, morphine, cocaine and tropane that stretching modes were assigned respectively to 3087, 3300, 3268, 3270, 2989 and 3280 cm^{-1} [1-3,5,7,9,17] while their hydrochloride species (hydrobromide in the scopolamine case) were assigned to

2316, 1882, 1746, 1776, 2089 and 1760 cm^{-1} [1-3,5,7,9,17]. The rocking modes in the two species of cyclizine were predicted between 1483 and 1402 cm^{-1}. Here, those modes were predicted between 1511 and 1463 cm^{-1}.

OH modes. The three species of naloxone have two O2-H37 and O4-H43 groups, for which, stretching, in-plane and torsion or out-of-plane deformation modes are expected for all species of naloxone. Thus, the two ATR bands at 3514 and 3418 cm^{-1} are assigned to those two O2-H37 and O4-H43 stretching modes because in the three species the SQM/B3LYP/6-31G* calculations predicted the two modes in that region [1-3,5,7,32,35,36]. The in-plane deformation modes in the free base are predicted between 1261 and 1216 cm^{-1} while in the cationic and hydrochloride species between 1253-1148 and 1303-1148 cm^{-1}, respectively. Hence, both modes can be assigned accordingly. The torsion or out-of-plane deformation modes for O4-H43 groups are predicted in the free base, cationic and hydrochloride species at 364, 366 and 368 cm^{-1} while for the other groups are predicted at 152, 177 and 22 cm^{-1}. Here, the presence of Cl in the hydrochloride form justifies the shifting of this mode to lower wavenumbers.

CH modes. Three aromatic C-H groups are present in the three structures of naloxone. Two C20-H40 and C22-H41 groups belong to rings D and one C23-H42 group belong to allyl chains, hence, the vibration modes expected for these groups are stretching modes and, in-plane and torsion or out-of-plane deformation modes. The C22-H41 stretching modes are predicted in the three species at higher wavenumbers than the other ones. Thus, the ATR and Raman bands between 3120 and 3015 cm^{-1} can be assigned to those stretching modes, as is detailed in Table 12. ATR and Raman bands between 1511 and 1149 cm^{-1} are assigned to in-plane deformation modes because they in the three species are predicted by calculations in those regions while the corresponding out-of-plane deformation modes are assigned, by the same reasons, to the bands between 1037 and 806 cm^{-1}, as observed in Table 12.

CH_2 modes. Structurally, the three species of naloxone have five CH_2 groups of which one of them belongs to allyl group where the C atoms of these $=CH_2$ groups have sp^2 hybridization different from the other ones with sp^3 hybridization. We can see from Table 12 that these groups are identified as $=CH_2$ (C24). Thus, the $=CH_2$ (C24) antisymmetric stretching modes are predicted by calculations at higher wavenumbers than the other ones and, where the symmetric stretching modes are characterized by Raman bands of media intensities, as shown in Table 12. The deformations modes of these groups can be assigned from 1471 cm^{-1} up to 1418 cm^{-1} because those modes are predicted for the three species in that region. The other wagging, rocking and twisting modes of those groups in cyclizine are assigned at 1477/1438, 1433/1360, 1319/1203 and 1037/766, respectively [17]. Here, these modes are attributed to the ATR and Raman bands at 1408/936, 1276/929 and 918/648 cm^{-1}, respectively, as predicted by SQM calculations. In the three species, the torsion modes τwCH_2(C24) are predicted in the same regions between 630 and 626 cm^{-1}, for which, they can be assigned to the strong ATR band at 648 cm^{-1}.

Skeletal modes. The N5-C19 stretching modes corresponding to allyl groups in the free base are predicted at 1120 cm^{-1} while in the cationic and hydrochloride species at 969 and 988 cm^{-1}, respectively. Thus, a very important difference with cyclizine (N-CH_3) is that those modes in the free base, cationic and hydrochloride species are predicted at 1160, 1035 and 1049 cm^{-1}, respectively [17]. In the three species of cocaine these stretching modes were predicted respectively at 1113, 1058 and 1052 cm^{-1} while in the tropane species are predicted at 1128, 1086 and 1031 cm^{-1} [1,2].

The very intense ATR band at 1707 cm^{-1}, in Raman observed weak at 1736 cm^{-1}, is clearly assigned to the C17=O3 stretching modes while the C23=C24 stretching modes of allyl chains in the three species can be also assigned at the same wavenumbers because the calculations predicted these modes in practically the same region. The other C=C stretching modes corresponding to D rings of three species are assigned to the ATR and Raman bands between 1646 and 1500 cm^{-1}. In relation to the five rings of all species of naloxone, for the A, C, D and E rings are expected three deformations and three torsions rings while for the B rings only two deformations and two torsions rings because these rings are of five members. In the three species, all these modes are predicted in the lower wavenumbers region and coupled among them [1-3,5,7,9,17]. The assignments of other remain skeletal modes were performed as predicted by calculations and, as shown in Table 12.

Force Fields.

The use of SQMFF methodology [27,28] and of Molvib program [29] allows us to calculate the harmonic force constants of the three species in both media which are of interest to know the different strengths of the bonds and justify in some cases the differences in their properties. Hence, the harmonic force constants were calculated for the three species of naloxone in gas phase and aqueous solution by using the corresponding harmonic force fields and the B3LYP/6-31G* method. Thus, in **Table 13** are presented the harmonic scaled force constants for the free base, cationic and hydrochloride species of naloxone in both media. Regarding the values of Table 13 it is observed that the *f(νN-H)* force constants for the cationic species don't not change in both media while the constant in gas phase for the hydrochloride species is lower than the corresponding in solution, a resulted also observed for morphine (2.73 and 4.61 mdyn $Å^{-1}$), cocaine (3.23 and 4.79 mdyn $Å^{-1}$) and tropane (2.70 and 4.69 mdyn $Å^{-1}$) alkaloids [1-3]. In the hydrochloride form of naloxone, the N-H distance is higher (1.087 Å) in gas phase than in aqueous solution (1.049 Å) justifying this way the differences between both force constants. A similar behaviour to those observed in the *f(νN-H)* force constants can be seen in the *f(νO-H)* force constants of hydrochloride species because in gas phase it is slightly higher than the value in solution. These differences can be explained by the average distances of the two O-H bonds because in gas phase the value is 0.981 Å while in solution is 0.972 Å. Hence, in solution the constant is higher than the value in gas phase. On the other hand, the three species present values *f(νC=O)* force constants higher in gas phase than in solution, as expected because the species are hydrated in this medium.

In relation to the $f(\nu N\text{-}C_{Allyl})$ force constants, in the free base the value is higher than in the cationic and hydrochloride species because the positive charges on the N atoms in these two forms produce diminishing in their values while these charges don't have not to influence on the $f(\nu C{=}C)_{Allyl}$ force constants.

Hence, in the three species those constants have practically the same values. Differences among the $f(\nu C\text{-}H)_R$ and $f(\nu C\text{-}H)_{Allyl}$ are not observed in the three species but the $f(\nu CH_2)$ and $(\nu CH_2)_{Allyl}$ force constants are different among them, hence, the values for the latter constants are higher than the other ones because these CH_2 groups belong to the allyl chains. However, the $f(\delta CH_2)_{Allyl}$ force constants in the three species are lower than the other $f(\delta CH_2)$ ones while the $f(\delta O\text{-}H)$ force constant for the hydrochloride species in gas phase is higher than the other ones and than that observed in the solution for this species.

Ultraviolet-visible spectra

The experimental available ultraviolet-visible spectrum of hydrochloride species of naloxone reported by Hassan et al [52] shows a maximum at 288 nm and a minimum at 268 nm. However, in the study performed by Mundhey et al [53] on hydrochloride species by using the Vierordt's method only an intense band at 283.8 nm is observed for that species in methanol solution. In this study, the B3LYP/6-31G* calculations predicted for the free base in aqueous solution an intense band at 240 nm and a shoulder at 310 nm while for the cationic and hydrochloride species only one intense band are predicted in both spectra respectively at 300 and 340 nm. The experimental spectrum published by Mundhey et al [53] for hydrochloride species of naloxone in methanol solution is compared in **Figure 9** with those predicted for the three species of naloxone in aqueous solution by using the B3LYP/6-31G* method. Both observed bands are assigned to $\pi\rightarrow\pi^*$ transitions due to the presence of C=C double bonds where the most intense band can be attributed to C=C double bonds of ring D [54,55] while that band of low intensity can be associated to allyl chain or to $n\rightarrow\pi^*$ transitions, as predicted by the NBO calculations.

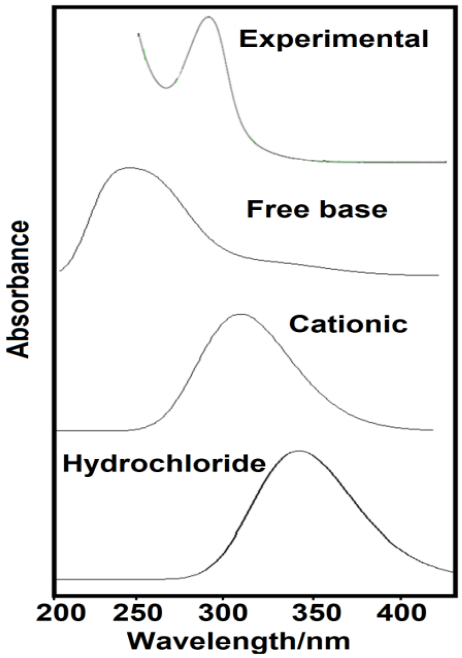

Figure 9. Experimental available spectrum for hydrochloride species of naloxone in methanol [53] compared with those predicted for the three species of naloxone in aqueous solution by using the B3LYP/6-31G* method.

Table 11. Global electrophilicity(ω) and nucleophilicity (E) indexes for the three species of naloxone compared with other species in gas and aqueous solution phases by using the B3LYP/6-31G* level of theory.

B3LYP/6-31G* method[a]				
FREE BASE				
Species	ω		E	
	Gas	PCM	Gas	PCM
Naloxone[a]	2.3233	2.3495	-7.4016	-7.6556
S(-)-Promethazine[b]	1.4911	1.4954	-6.2524	-6.3701
R(+)-Promethazine[b]	1.4845	1.4912	-6.3578	-6.4266
Cyclizine[c]	1.6777	1.7288	-8.1146	-8.4953
Morphine[d]	1.3639	1.2339	-7.7475	-7.1153
Cocaine[e]	2.5183	2.5297	-8.4959	-8.7546
Scopolamine[#,f]	1.7393	1.7504	-8.2756	-8.4763
Heroin[g]	1.5083	1.5180	-8.2606	-8.2545
Tropane[f,h]	0.3914	0.4429	-6.4905	-7.0557
CATIONIC				
Naloxone[a]	8.2495	8.2594	-14.8727	-15.1620
S(-)-Promethazine[b]	7.0158	I	-12.9219	I
R(+)-Promethazine[b]	6.9790	2.0092	-12.9341	-7.6061
Cyclizine[c]	6.5083	I	-16.8238	I
Morphine[d]	6.8155	6.9811	-15.4288	-14.8785
Cocaine[e]	7.9799	7.7229	-17.9548	-17.7568
Scopolamine[#,f]	6.4529	6.2963	-16.9925	-16.7551
Heroin[g]	6.7459	6.9284	-16.4174	-16.4035
Tropane[f,h]	6.9598	7.0263	-38.9872	-38.9613
HYDROCHLORIDE				
Naloxone[a]	2.4641	3.1887	-8.9709	-4.5667
S(-)-Promethazine[b]	2.0092	2.0184	-7.6061	-6.1234

R(+)-Promethazine[b]	1.8118	1.8817	-7.1020	-6.5311
Cyclizine[c]	I	1.9053	I	-5.9742
Morphine[d]	1.8476	1.8414	-8.6274	-6.6589
Cocaine[e]	2.6244	2.6828	-7.7534	-5.7845
Scopolamine[#,f]	1.7421	0.9799	-7.2107	-6.2154
Heroin[g]	1.9711	1.9667	-8.5711	-6.5755
Tropane[f,h]	0.6955	0.6421	-7.4343	-5.7592

[#]Hydrobromide, [a]This work, [b]From Ref [8], [c]From Ref [17], [d]From Ref [1], [e]From Ref [3], [f]From Ref [7], [g]From Ref [5], [h]From Ref [2]. I=imaginary frequencies

Table 12. Observed and calculated wavenumbers (cm^{-1}) and assignments for the free base, cationic and hydrochloride species of naloxone in gas phase

Experimental[d]		B3LYP/6-31G* Method[a]					
Hydrochloride		Free base		Cationic		Hydrochloride	
ATR[c]	Raman[c]	SQM[b]	Assignments	SQM[b]	Assignments	SQM[b]	Assignments
3514m		3589	νO2-H37	3604	νO2-H37	3567	νO4-H43
3418m		3571	νO4-H43	3570	νO4-H43	3215	νO2-H37
3140sh				3221	νN5-H46	3112	ν_aCH_2(C24)
3120m	3097w	3102	ν_aCH_2(C24)	3126	ν_aCH_2(C24)	3083	νC22-H41
3068m	3073w	3079	νC22-H41	3091	νC22-H41	3063	νC23-H42
3056m	3049w	3052	νC20-H40	3065	νC20-H40	3055	νC20-H40
				3042	ν_sCH_2(C24)	3033	ν_aCH_2(C14)
3025m	3039w			3039	ν_aCH_2(C14)	3028	ν_sCH_2(C24)
	3015sh	3034	νC23-H42	3036	νC23-H42	3009	ν_aCH_2(C19)
	3007w	3023	ν_sCH_2(C24)	3023	ν_aCH_2(C19)	3004	ν_aCH_2(C16)
3004sh				3010	ν_aCH_2(C16)	2996	ν_aCH_2(C12)
2997m	2996sh	2994	ν_aCH_2(C16)	2998	ν_aCH_2(C10)	2994	ν_aCH_2(C10)
		2989	ν_aCH_2(C12)	2994	ν_aCH_2(C12)	2980	νC9-H26
2973sh	2984m	2985	ν_aCH_2(C10)	2985	ν_sCH_2(C14)	2974	ν_sCH_2(C14)
	2975m	2963	ν_aCH_2(C14)	2974	νC8-H25	2970	νC8-H25
		2956	νC9-H26	2964	νC9-H26	2961	ν_aCH_2(C13)
2953sh	2953m	2944	ν_sCH_2(C12)	2959	ν_sCH_2(C19)	2951	ν_sCH_2(C12)
2941sh		2940	ν_sCH_2(C10)	2952	ν_sCH_2(C10)	2949	ν_sCH_2(C10)
	2932m	2939	ν_aCH_2(C13)	2949	ν_sCH_2(C12)	2943	ν_sCH_2(C16)
		2931	νC8-H25	2945	ν_aCH_2(C13)	2943	ν_sCH_2(C19)
2929sh		2911	ν_aCH_2(C19)	2921	ν_sCH_2(C13)	2922	ν_sCH_2(C13)
2913sh	2906sh	2896	ν_sCH_2(C13)	2893	ν_sCH_2(C16)		
2841w	2868w	2889	ν_sCH_2(C16)				
		2823	ν_sCH_2(C14)				
		2805	ν_sCH_2(C19)				
						2312	νN5-H46
1707vs	1736w	1757	νC17-O3	1775	νC17-O3	1757	νC17-O3
	1720w	1664	νC23-C24	1661	νC23-C24	1664	νC23-C24
1631m	1646s	1636	νC11-C18	1634	νC11-C18	1634	νC11-C18
1609m		1611	νC11-C15,νC18-C21	1608	νC11-C15	1610	νC11-C15
1500m	1513w	1505	νC21-C22	1509	νC21-C22	1511	ρN5-H46,τN5-H46
1471m	1467sh	1476	δCH_2(C14)			1481	ρ'N5-H46
1459m	1457w			1463	ρ'N5-H46	1461	δCH_2(C13)
1459m	1457w			1457	δCH_2(C14)	1459	δCH_2(C10)
1459m	1457w	1451	δCH_2(C12) δCH_2(C13)	1450	δCH_2(C12)	1454	δCH_2(C14)
1443s	1440sh	1448	δCH_2(C19)	1448	δCH_2(C19)		
1443s	1440sh			1448	δCH_2(C12)		
		1446	δCH_2(C12)	1443	δCH_2(C13)	1446	βR_2(A3)νC11-C18
1443s	1440sh	1441	δCH_2(C16)	1440	δCH_2(C16)	1446	δCH_2(C12)
	1432sh	1439	δCH_2(C10)	1437	δCH_2(C16)	1441	δCH_2(C19)
1428w	1426m	1434	δCH_2(C13)	1420	δCH_2(C24)	1425	δCH_2(C16)
1418m		1424	δCH_2(C24)	1417	ρN5-H46	1420	δCH_2(C24)
1408w	1389w	1405	wagCH_2(C14)	1385	wagCH_2(C14)	1394	wagCH_2(C14)
1378m	1368sh	1384	ρ'C8-H25	1380	wagCH_2(C10)	1382	wagCH_2(C19)
1372sh	1362w	1369	wagCH_2(C12)	1371	wagCH_2(C13)	1372	wagCH_2(C12)
		1361	wagCH_2(C13)	1367	wagCH_2(C12)	1362	wagCH_2(C13)

Experimental[d]		B3LYP/6-31G* Method[a]					
Hydrochloride		Free base		Cationic		Hydrochloride	
1356sh	1356sh	1357	$wagCH_2$(C19)	1358	$wagCH_2$(C10)	1359	$wagCH_2$(C10)
1346sh		1350	$wagCH_2$(C10)	1349	ρ'C8-H25	1345	ρ'C8-H25
1340w	1338w	1343	νC11-C15,βC20-H40	1345	νC11-C15	1343	$wagCH_2$(C19)
				1333	$wagCH_2$(C16)	1336	$wagCH_2$(C16)
1328w		1326	$wagCH_2$(C16),ρCH_2(C12)	1328	βC22-H41		
1320w	1318sh	1321	νC18-O1	1318	ρ'C9-H26	1322	νC20-C22
1310m	1310m	1316	ρ'C9-H26			1314	ρ'C9-H26
	1300sh			1304	ρC23-H42	1303	δO2-H37
1296w		1293	ρ'C9-H26	1299	ρC8-H25	1296	ρC23-H42
1290sh	1286w	1290	ρC8-H25			1292	$wagCH_2$(C16)
		1285	ρC23-H42	1285	ρC9-H26	1281	ρC9-H26
1276w	1266w	1276	ρC9-H26	1273	ρCH_2(C10)	1272	ρCH_2(C19)
1262sh		1261	δO2-H37	1253	δO2-H37,νC7-C8		
1256m	1245w	1258	ρCH_2(C19)	1249	ρCH_2(C19)	1251	ρCH_2(C19)
1238sh	1236sh	1236	ρCH_2(C10)	1234	ρCH_2(C16)	1244	ρCH_2(C16)
1230sh	1231sh	1231	ρCH_2(C14)	1231	βR_1(A4),νC18-O1	1231	ρCH_2(C14)
1225s		1219	ρCH_2(C13)	1222	ρCH_2(C13)	1228	ρCH_2(C13)
1211s	1207m	1216	βR_1(A4),δO4-H43	1213	βR_1(A4)	1215	βR_1(A4)ρC9-H26
1197sh	1194w	1201	ρCH_2(C16)	1198	ρCH_2(C13)	1201	ρCH_2(C10)
1189sh		1185	βR_2(A5)	1184	ρCH_2(C16)	1183	ρC8-H25
1179s	1177w	1165	βR_1(A5), ρCH_2(C12)	1170	νC7-C12	1166	νC6-C11
1161sh	1168sh	1153	νC6-C11	1158	βC22-H41	1154	βC22-H41
1145sh	1149sh	1149	βC22-H41,νC20-C22	1148	δO4-H43,νC6-C11	1148	δO4-H43
1139m	1142sh	1139	βR_1(A5)			1135	βR_1(A5),ρCH_2(C24)
		1120	νN5-C19	1128	βR_1(A5),ρCH_2(C24)		
1105s	1117w	1111	νN5-C14	1100	βR_1(A5)νC6-C9	1106	βR_1(A5), νC6-C9
1089sh	1095w	1098	νC16-C17,βC17-O3	1093	νC16-C17	1104	νC16-C17
		1084	νC6-C7	1083	τR_1(A1), νC6-C7	1097	νC6-C7
1079sh	1063w	1077	νC6-C9	1065	νC6-C10,βR_1(A1)	1076	νC6-C10,βR_1(A1)
1049s	1054sh	1057	νC6-C10,βR_1(A1)			1049	νC7-O2
1039sh	1034sh					1037	γC23-H42
1022s	1026sh	1027	νC7-O2	1034	νC8-C13	1031	νC7-C8,ρ'C7-O2
		1019	γC23-H42,τR_1(A1)	1016	τR_1(A1),νC7-O2	1018	νN5-C14
1010w	1018m	1012	γC23-H42,νC7-C8	1005	νC10-C14	1002	νC8-C13
992m	1004w	1002	νC13-C15	998	νC13-C15,βR_2(A2)		
	994sh			996	$wagCH_2$(C24)		
				993	$wagCH_2$(C24)	988	νN5-C19
976sh	978w	978	νC10-C14	986	νC10-C14νN5-C14	977	τR_2(A5)
966w	962sh	969	νC9-O1	969	νN5-C19	971	νC10-C14
946s	956w	952	νC12-C16,νC8-C13	959	νC9-O1	959	$wagCH_2$(C24)
	930w	937	$wagCH_2$(C24)	947	γC20-H40	958	$wagCH_2$(C24)
940sh		936	$wagCH_2$(C24)	940	γC22-H41	940	νC12-C16
926sh		926	νC19-C23	932	νC12-C16	930	νC19-C23
	916sh	924	γC20-H40	929	νC19-C23	923	γC20-H40
918s		921	γC22-H41,γC20-H40	913	νC7-O2	921	νC8-C13
900sh	906sh	903	τwCH_2(C13)	900	βR_2(A3)	901	νC9-O1
896m	894sh	894	βR_2(A2),τwCH_2(C16)	890	τR_1(A3)	897	βR_2(A2)
	874sh	885	ρCH_2(C24)	886	τwCH_2(C13)	889	τwCH_2(C13)
868w	853w	861	τwCH_2(C19)				
845m	823sh			837	τwCH_2(C19)	843	τwCH_2(C19)
817sh	813w	824	βR_1(A4), τwCH_2(C12)	818	γC20-H40	818	τwCH_2(C12)
807sh	807w	810	γC22-H41	814	γC20-H40,βR_1(A4)	808	νC9-C17
799s	783w	799	νC9-C17,τwCH_2(C12)	798	νC9-C17	806	γC22-H41
771w	773sh	783	τwCH_2(C14)				
760sh	767sh	765	νN5-C14,νN5-C8	773	νN5-C14	775	νN5-C14
	761sh			753	νN5-C8	759	νN5-C8,τwCH_2(C14)
737m	747w	733	τwCH_2(C10)	731	τwCH_2(C10)	747	τwCH_2(C10)
731sh	707m	722	τR_1(A4), τR_2(A4)	713	τR_1(A4)	719	τR_1(A4)

Experimental[d]		B3LYP/6-31G* Method[a]					
Hydrochloride		Free base		Cationic		Hydrochloride	
699sh	687w	695	βR_2(A4)	692	βR_2(A4)	696	βR_3(A4), βR_2(A4)
679w	679sh	678	τR_1(A4), βR_3(A3)	674	τR_1(A4),βR_3(A3)	677	τR_1(A4), βR_3(A3)
648s	655sh	626	τwCH_2(C24)	630	τwCH_2(C24)	630	τwCH_2(C24)
624s	632s	621	γC17-O3	623	βR_2(A2)	621	βR_2(A2)
602s	616vs	613	τR_1(A4)	613	γC21-O4	612	τR_1(A4)
	588m	592	βR_2(A2)	591	γC21-O4	599	γC21-O4
586sh		584	γC21-O4	583	τR_2(A4)	585	τR_2(A4)
						580	ρC7-O2,δC8N5C19
576s	574sh	577	βR_2(A3)	573	βC17-O3	577	βR_2(A3)
566sh	556w	564	ρC7-O2	563	ρC7-O2	551	τR_3(A4), τR_2(A2)
546m		546	τR_3(A4), τR_2(A2)	544	τR_3(A4), τR_2(A2)	532	βR_1(A5), βR_2(A5)
514w	510sh	525	βR_2(A5),βR_1(A5)	518	βR_1(A5)	514	βC17-O3,βR_3(A1)
504sh	498m	506	βR_2(A5)	508	βR_2(A5)βR_1(A5)	503	βR_3(A5)
488w	476sh	485	βR_3(A5)	497	βR_3(A5)	490	βR_2(A5)
457w	468m	464	βR_3(A4)	468	βR_3(A4)	465	τR_3(A3), τR_3(A5)
	459sh	450	γN5-C19	455	δC19C23C24	459	βR_3(A4)
425sh	419sh	424	βR_3(A4),βR_2(A3)	423	δC19C23C24	426	δC19C23C24
403s	409s	419	δC19C23C24,βN5-C19	411	βR_3(A4)	411	τR_1(A1), βR_3(A4)
	385sh	403	βR_2(A3),βR_2(A1)	402	βR_2(A3)	407	βR_2(A3), βR_2(A1)
	371sh			376	βR_2(A5)	379	βR_2(A5),δC14N5C19
	365m	364	τO4-H43,τR_1(A3)	366	τO4-H43	368	τO4-H43
	361m	360	βR_2(A5), ρ'C7-O2	358	τR_1(A3), τR_3(A3)	360	τR_1(A3)
	349m	353	τO4-H43	352	ρC7-O2	352	τR_3(A3), τR_2(A3)
	345sh	340	τR_3(A3), τR_2(A5)			342	τR_3(A3), βR_2(A3)
	329m	339	τR_3(A3), τR_1(A3)	336	τR_3(A3), τR_1(A3)	320	τR_2(A3), τR_1(A5)
	319w	313	τR_1(A5), βR_2(A5)	317	τR_1(A2)		
	301w					301	τR_1(A5)
	293w	289	δC23C19N5	288	ρ'C7-O2	291	τR_1(A1)
	279sh	274	τR_1(A3), τR_1(A5)	277	τR_2(A3)	278	τR_1(A5), τR_1(A1)
	271sh	272	τR_2(A3), βR_3(A1)	273	τR_1(A5)	261	τR_3(A1)
	261m	256	τR_1(A1), τR_2(A3)	249	τR_2(A3), τR_1(A1)		
	238w	244	βR_3(A3), βC21-O4	241	βC21-O4,βR_3(A3)	241	τR_2(A3),δC23C19N5
	224sh	221	τR_3(A5)	228	τR_3(A3),τR_2(A3)	239	βC21-O4
	208sh	221	τR_2(A3), βR_2(A3)	221	τR_3(A5),βR_2(A3)	215	τR_3(A5)
	192s					198	νH46-Cl47
	176sh			177	τO2-H37,τR_3(A1)		
		168	τR_3(A1)	160	τR_2(A1),τR_3(A5)	166	τR_2(A1),τR_3(A5)
		152	τO2-H37	152	τR_1(A3)	153	τR_3(A3), τR_2(A1)
		149	τR_2(A3), τO2-H37			124	τR_1(A1), τR_2(A1)
		116	τR_3(A3), τR_2(A5)	113	τR_2(A1), τR_3(A3)	112	τR_3(A3), τR_2(A5)
		96	τR_2(A5), τC19-N5	96	τR_3(A5),τR_2(A5)	105	τR_2(A5)
		77	τC23-C19	74	τR_3(A3)	75	τC23-C19
						72	τR_3(A3),τC19-N5
		67	τR_3(A3)	65	τC23-C19		
		57	τR_2(A1),τR_1(A1)	60	τR_2(A1)	57	τR_2(A1),τR_1(A1)
		41	τR_3(A3),τR_2(A3)			46	τR_2(A1), τR_3(A3)
				38	τC19-N5		
						22	τO2-H37

Abbreviations: ν, stretching; δ, deformation in the plane; γ, deformation out of plane; wag, wagging; τ, torsion; β_R, deformation ring τ_R, torsion ring; ρ, rocking; τw, twisting; δ, deformation; a, antisymmetric; s, symmetric; (A_1), Ring A; (A_2), Ring B; (A_3), Ring C; (A_4), Ring D; (A_5), Ring E.
[a]This work, [b]From scaled quantum mechanics force field; [c]From Ref [30]; [d]From Ref [30] for hydrochloride dihydrated in solid phase.

Table 13. Scaled internal force constants for the free base, cationic and hydrochloride naloxone species in gas and aqueous solution phases by using the B3LYP/6-31G* method.

Force constant	Naloxone[a]					
	Free base		Cationic		Hydrochloride	
	Gas	PCM	Gas	PCM	Gas	PCM

f(νN-H)			5.75	5.74	3.83	5.09
f(νO-H)	7.17	7.16	7.20	7.15	6.43	7.17
f(νC=O)	12.47	11.52	12.76	11.63	12.45	11.60
f(νN-C$_{Allyl}$)	4.68	4.56	3.51	3.68	3.80	3.69
f(νC=C)$_R$	5.72	5.70	7.33	7.34	7.33	7.33
f(νC=C)$_{Allyl}$	9.18	9.12	9.15	9.19	9.19	9.15
f(νC-N)	4.91	4.73	3.86	4.04	4.14	4.03
f(νCH$_2$)	4.72	4.77	4.87	4.92	4.88	4.93
f(νCH$_2$)$_{Allyl}$	5.16	5.15	5.22	5.20	5.17	5.17
f(νC-H)$_R$	5.16	5.18	5.20	5.19	5.17	5.19
f(νC-H)$_{Allyl}$	5.06	5.04	5.05	5.08	5.15	5.14
f(δCH$_2$)	0.74	0.73	0.74	0.73	0.74	0.73
f(δCH$_2$)$_{Allyl}$	0.44	0.43	0.44	0.43	0.44	0.44
f(δO-H)	0.74	0.79	0.71	0.77	0.83	0.77

Units are mdyn Å^{-1} for stretching and mdyn Å rad^{-2} for angle deformations
[a]This work

4. CONCLUSIONS

The functional hybrid B3LYP and the 6-31G* basis set were used to determine the theoretical structures of free base, cationic and hydrochloride species of naloxone in gas phase and in aqueous solution. The species in solution were optimized employing the SCRF methodology and the PCM method while the solvation energies were computed with the universal solvation model.

The SQMFF methodology and the Molvib program were used to compute the harmonic force fields of three species in the two media while the complete vibrational assignments of bands observed in the experimental ATR and Raman spectra were performed by using the harmonic force fields and the normal internal coordinates. Hence, the expected 129, 132 and 135 vibration normal modes for the free base, cationic and hydrochloride species of naloxone, respectively are reported.

The free base of naloxone evidence the higher solvation energy value, as compared with those reported for S(-)-promethazine, R(+)-promethazine, cyclizine, morphine, cocaine, scopolamine, heroin, and tropane alkaloids. The solvation energy value for the cationic species (-302.45 kJ/mol) is closer to that observed for morphine (-309.19 kJ/mol) while the value for the hydrochloride species (-122.28 kJ/mol) is near to scopolamine value (-122.74 kJ/mol).

The AIM analyses show ionic characteristic of N-H···Cl bonds in the hydrochloride species and suggest that this species in both media is as cationic one, as supported by the positive MK charges on the N5 atoms in the hydrochloride species in both media and by the absence in the ATR spectrum of band at 2405 cm^{-1}, associated to N5-H46 stretching mode.

Moreover, frontier orbitals studies evidence that the allyl chains present in the three species of naloxone diminishing the gap values increasing their reactivities, as compared with the other species containing the N-CH$_3$ group.

The *f(νN-H)* force constants for the hydrochloride species are lower than the corresponding in solution, a result also observed for morphine (2.73 and 4.61 mdyn Å^{-1}), cocaine (3.23 and 4.79 mdyn Å^{-1}) and tropane (2.70 and 4.69 mdyn Å^{-1}) alkaloids.

Comparisons between experimental infrared, Raman and ultraviolet-visible spectra with the corresponding predicted show good correlations.

5. REFERENCES

1. Brandán, S.A. Why morphine is a molecule chemically powerful. Their comparison with cocaine. *Indian Journal of Applied Research* **2017**, *7*, 511-528.
2. Rudyk, R.A.; Brandán, S.A. Force field, internal coordinates and vibrational study of alkaloid tropane hydrochloride by using their infrared spectrum and DFT calculations. *Paripex A Indian Journal of Research* **2017**, *6*, 616-623.
3. Romani, D.; Brandán, S.A. Vibrational analyses of alkaloid cocaine as free base, cationic and hydrochloride species based on their internal coordinates and force fields. *Paripex A Indian Journal of Research* **2017**, *6*, 587-602.
4. Iramain, M.A.; Ledesma, A.E.; Brandán, S.A. Analyzing the effects of halogen on properties of a halogenated series of R and S enantiomers analogues alkaloid cocaine-X, X=F, Cl, Br, I. *Paripex A Indian Journal of Research* **2017**, *6,* 454-463.
5. Brandán, S.A. Understanding the potency of heroin against to morphine and cocaine. *International Journal of Science and Research Methodology* **2018**, *12*, 97-140.
6. Rudyk, R.A.; Checa, M.A.; Guzzetti, K.A.; Iramain, M.A.; Brandán, S.A. Behaviour of N-CH$_3$ Group in Tropane Alkaloids and correlations in their Properties. *International Journal of Science And Research Methodology* **2018**, *10,* 70-97.
7. Rudyk, R.A.; Checa, M.A.; Catalán, C.A.N.; Brandán, S.A. Structural, FT-IR, FT-Raman and ECD spectroscopic studies of free base, cationic and hydrobromide species of scopolamine alkaloid. *J. Mol. Struct*. **2019**, *1180*, 603-617. https://doi.org/10.1016/j.molstruc.2018.12.040.
8. Manzur, M.E.; Brandán, S.A. S(-) and R(+) Species Derived from Antihistaminic Promethazine Agent: Structural and Vibrational Studies. *Heliyon* **2019**, *5,* e02322, https://doi.org/10.1016/j.heliyon.2019.e02322.
9. Brandán, S.A. Structural and Vibrational Studies of Equilenin, Equilin and Estrone Steroids. *Biointerface Research in Applied Chemistry* **2019**, 9, 4502-4516, https://doi.org/10.33263/BRIAC96.502516.
10. Iramain, M.A.; Davies, L.; Brandán, S.A. FTIR, FT-Raman and UV-visible spectra of Potassium 3-furoyltrifluoroborate. *J. Mol. Struct.* **2018**, *1158,* 245-254, https://doi.org/10.1016/j.molstruc.2018.01.040

11. Kausteklis, J.; Aleksa, V.; Iramain, M.A.; Brandán, S.A. Cation-anion interactions in 1-buthyl-3-methyl imidazolium nitrate ionic liquid and their effect on their structural and vibrational properties. *J Mol. Struct*. **2018**, *1164,* 1-14, https://doi.org/10.1016/j.molstruc.2018.03.100.
12. Iramain, M.A.; Davies, L.; Brandán, S.A. Evaluating structures, properties and vibrational and electronic spectra of the potassium 2-isonicotinoyltrifluoroborate salt. *J. Mol. Struct*. **2018**, *1163*, 41-53, https://doi.org/10.1016/j.molstruc.2018.02.098.
13. Kausteklis, J.; Aleksa, V.; Iramain, M.A.; Brandán, S.A. DFT study and vibrational assignment of 1-Butyl-3-methylimidazolium trifluoromethanesulfonate ionic liquid by using the FT-Raman spectrum, *J Mol. Struct.* **2019**, 1175, 663-676, https://doi.org/10.1016/j.molstruc.2018.08.014.
14. Iramain, M.A.; Davies, L.; Brandán, S.A. Structural and spectroscopic differences among the Potassium 5-hydroxypentanoyltrifluoroborate salt and the furoyl and isonicotinoyl salts. *J Mol. Struct*. **2019**, *1176*, 718-728, https://doi.org/10.1016/j.molstruc.2019.02.010.
15. Iramain, M.A.; Ledesma, A.E.; Brandán, S.A. Structural properties and vibrational analysis of Potassium 5-Br-2-isonicotinoyltrifluoroborate salt. Effect of Br on the isonicotinoyl ring, *J Mol. Struct*. **2019**, 1184, 146-156, https://doi.org/10.1016/j.molstruc.2019.02.010.
16. Iramain, M.A.; Brandán, S.A. Structural and vibrational properties of three species of anti-histaminic diphenhydramine by using DFT calculations and the SQM approach. *To Chemistry Journal* **2018**, *1*, 105-130.
17. Márquez, M.J.; Iramain, M.A.; Brandán, S.A. *Ab-initio* and Vibrational studies on Free Base, Cationic and Hydrochloride Species Derived from Antihistaminic Cyclizine agent, IJSRM. *International Journal of Science and Research Methodology* **2018**, *12*, 97-140.
18. Karle, I.L. On the Conformation of Naloxone, a Narcotic Antagonist. *Acta Cryst.* **1974**, *B30*, 1682-1686.
19. Wermeling, D.P. Review of naloxone safety for opioid overdose: practical considerations for new technology and expanded public Access. *Ther Adv Drug Saf* **2015**, *6*, 20–31, https://doi.org/10.1177/2042098614564776.
20. Pert, C.B.; Pasternak, G.; Snyder, S.H. Opiate agonists and antagonists discriminated by receptor binding in brain. *Science* **1973**, *182,* 1359-1361, https://doi.org/10.1126/science.182.4119.1359.
21. Pert, C.B.; Snyder, S.H. Opiate receptor: demonstration in nervous tissue. *Science* **1973**, *179,* 1011-1014, https://doi.org/10.1126/science.179.4077.1011
22. Lee C, Yang W, Parr RG. Development of the Colle-Salvetti correlation-energy formula into a functional of the electron density. *Phys. Rev*. **1988**, *B37,* 785-789.
23. Becke, A.D. Density-functional exchange-energy approximation with correct asymptotic behavior. *Phys. Rev*. **1988**, *A38*, 3098-3100, https://doi.org/10.1103/PhysRevA.38.3098.
24. Miertus, S.; Scrocco, E.; Tomasi, J. Electrostatic interaction of a solute with a continuum. *Chem. Phys.* **1981,** *55*, 117–129, https://doi.org/10.1016/0301-0104(81)85090-2.
25. Tomasi, J.; Persico, J. Molecular Interactions in Solution: An Overview of Methods Based on Continous Distributions of the Solvent. *Chem. Rev*. **1994**, *94,* 2027-2094, https://doi.org/10.1021/cr00031a013.
26. Marenich, A.V.; Cramer, C.J.; Truhlar, D.G. Universal solvation model based on solute electron density and a continuum model of the solvent defined by the bulk dielectric constant and atomic surface tensions. *J. Phys. Chem.* **2009**, *B113*, 6378-6396, https://doi.org/10.1021/jp810292n.
27. Pulay, P.; Fogarasi, G.; Pongor, G.; Boggs, J.E.; Vargha, A. Combination of theoretical ab initio and experimental information to obtain reliable harmonic force constants. Scaled quantum mechanical (QM) force fields for glyoxal, acrolein, butadiene, formaldehyde, and ethylene. *J. Am. Chem. Soc*. **1983**, *105,* 7073, https://doi.org/10.1021/ja00362a005.
28. Rauhut, G.; Pulay, P. Transferable Scaling Factors for Density Functional Derived Vibrational Force Fields. *J. Phys. Chem*. **1995**, *99*, 3093-3100, https://doi.org/10.1021/j100010a019.
29. Sundius, T. Scaling of ab-initio force fields by MOLVIB. *Vib. Spectrosc*. **2002**, *29,* 89-95, https://doi.org/10.1016/S0924-2031(01)00189-8.
30. *Experimental available ATR and Raman spectra from:* https://spectrabase.com/spectrum/
31. Paar, R.G.; Pearson, R.G. Absolute hardness: companion parameter to absolute electronegativity. *J. Am. Chem*. Soc. **1983**, *105*, 7512-7516, https://doi.org/10.1021/ja00364a005.
32. Minteguiaga, M.; Dellacassa, E.; Iramain, M.A.; Catalán, C.A.N.; Brandán, S.A. Synthesis, spectroscopic characterization and structural study of 2-isopropenyl-3-methylphenol, carquejiphenol, a carquejol derivative with potential medicinal use. *J Mol. Struct*. **2018**, *1165*, 332-343, https://doi.org/10.1016/j.molstruc.2018.04.001.
33. M'leh, B.C.; Brandán, S.A.; Issaoui, N.; Roisnel, T.; Marouani, H. Synthesis, molecular structure, vibrational and theoretical studies of a new non-centrosymmetric organic sulphate with promising NLO properties. *J Mol. Struct.* **2018**, 1171, 771-785, https://doi.org/10.1016/j.molstruc.2018.06.041.
34. Gatfaoui, S.; Issaoui, N.; Brandán, S.A.; Roisnel, T.; Marouani, H. Synthesis and characterization of p-xylylenediaminiumbis(nitrate). Effects of the coordination modes of nitrate groups on their structural and vibrational properties. *Journal of Molecular Structure* **2018**, *1151*, 152-168, http://dx.doi.org/10.1016/j.molstruc.2017.09.027.
35. Minteguiaga, M.; Dellacassa, E.; Iramain, M.A.; Catalán, C.A.N.; Brandán, S.A. FT-IR, FT-Raman, UV-Vis, NMR and structural studies of Carquejyl Acetate, a component of the essential oil from *Baccharis trimera* (Less.) DC. (Asteraceae). *J Mol. Struct*. **2019**, *1177*, 499-510, https://doi.org/10.1016/j.molstruc.2018.10.010.
36. Ruiz Hidalgo, J.; Neske, A.; Iramain, M.A.; Alvarez, P.E.; Leyton Bongiorno, P.; Brandán, S.A. FT-IR, FT-Raman and UV-visible spectra of motrilin acetogenin isolated from *Annona cherimolia. J Mol. Struct.* **2019**, *1196,* 508-517, https://doi.org/10.1016/j.molstruc.2019.06.107
37. Trabelsi, S.; Issaoui, N.; Brandán, S.A.; Bardak, F.; Roisnel, T.; Atac , A.; Marouani, H. Synthesis and physic-chemical properties of a novel chromate compound with potential biological applications, bis(2-phenylethylammonium) chromate(VI), *J Mol. Struct.* **2019**, *1185,* 168-182, https://doi.org/10.1016/j.molstruc.2019.02.106.
38. Iramain, M.A.; Castillo, M.V.; Davies, L.; María E. Manzur, M.E.; Brandán, S.A. Structural and SQMFF study of potent insecticide 40,40-DDT combining the FT-IR and FT-Raman spectra with DFT calculations. *J. Mol. Struct.* **2020**, *1199,* 126964, https://doi.org/10.1016/j.molstruc.2019.126964.
39. Kausteklis, J.; Aleksa, V.; Iramain, M.A.; Brandán, S.A. DFT study and vibrational assignment of 1-Butyl-3-methylimidazolium trifluoromethanesulfonate ionic liquid by using the FT-Raman spectrum. *J. Mol. Struct.* **2019**, *1175*, 663-676, https://doi.org/10.1016/j.molstruc.2018.08.014.
40. Iramain, M.A.; Davies, L.; Brandán, S.A. Structural and spectroscopic differences among the Potassium 5-hydroxypentanoyltrifluoroborate salt and the furoyl and isonicotinoyl salts. *J Mol. Struct*. **2019**, *1176*, 718-728, https://doi.org/10.1016/j.molstruc.2018.09.015.

41. Nielsen, A.B.; Holder, A.J. *Gauss View 3.0. User's Reference,* Gaussian Inc., Pittsburgh, PA, **2000–2003**.
42. Frisch, M.J.; Trucks, G.W.; Schlegel, H.B.; Scuseria, G.E.; Robb, M.A.; Cheeseman, J.R.; Scalmani, G.; Barone, V.; Mennucci, B.; Petersson, G.A.; Nakatsuji, H.; Caricato, M.; Li, X.; Hratchian, H.P.; Izmaylov, A.F.; Bloino, J.; Zheng, G.; Sonnenberg, J.L.; Hada, M.; Ehara, M.; Toyota, K.; Fukuda, R.; Hasegawa, J.; Ishida, M.; Nakajima, T.; Honda, Y.; Kitao, O.; Nakai, H.; Vreven, T.; Montgomery, J.A.; Peralta, J.E.; Ogliaro, F.; Bearpark, M.; Heyd, J.J.; Brothers, E.; Kudin, K.N.; Staroverov, V.N.; Kobayashi, R.; Normand, J.; Raghavachari, K.; Rendell, A.; Burant, J.C.; Iyengar, S.S.; Tomasi, J.; Cossi, M.; Rega, N.; Millam, J.M.; Klene, M.; Knox, J.E.; Cross, J.B.; Bakken, V.; Adamo, C.; Jaramillo, J.; Gomperts, R.; Stratmann, R.E.; Yazyev, O.; Austin, A.J.; Cammi, R.; Pomelli, C.; Ochterski, J.W.; Martin, R.L.; Morokuma, K.; Zakrzewski, V.G.; Voth, G.A.; Salvador, P.; Dannenberg, J.J.; Dapprich, S.; Daniels, A.D.; Farkas, O.; Foresman, J.B.; Ortiz, J.; Cioslowski, J.; Fox, D.J. Gaussian, Inc., Wallingford CT, **2009**.
43. Ugliengo, P. *Moldraw Program*. University of Torino, Dipartimento Chimica IFM, Torino, Italy, **1998**.
44. Glendening, E.; Badenhoop, J.K.; Reed, A.D.; Carpenter, J.E.; Weinhold, F. NBO 3.1; *Theoretical Chemistry Institute, University of Wisconsin; Madison,* WI, 1996.
45. Biegler-Köning, F.; Schönbohm, J.; Bayles, D. AIM2000; A Program to Analyze and Visualize Atoms in Molecules. *J. Comput. Chem.* **2001**, *22*, 545, http://dx.doi.org/10.1002/1096-987X(20010415)22:5%3C545::AID-JCC1027%3E3.0.CO;2-Y.
46. Gylbert, L. The Crystal and Molecular Structure of Morphine Hydrochloride Trihydrate. *Acta Cryst.* **1973**, *B29*, 1630, https://doi.org/10.1107/S0567740873005169.
47. Gelbrich, T.; Braun, D.E.; Griesser, U.J. Morphine hydrochloride anhydrate. *Acta Cryst.* **2012**, *E68*, o3358–o3359, https://doi.org/10.1107/S1600536812046405.
48. Gelbrich, T.; Braun, D.E.; Griesser, U.J. Stable polymorph of morphine. *Acta Cryst.* **2013**, *E69*, o2, https://doi.org/10.1107/S1600536812048945.
49. Bader, R.F.W. *Atoms in Molecules, A Quantum Theory.* Oxford University Press, Oxford, 1990.
50. Keresztury, G.; Holly, S.; Besenyei, G.; Varga, J.; Wang, A.Y.; Durig, J.R. Vibrational spectra of monothiocarbamates-II. IR and Raman spectra, vibrational assignment, conformational analysis and ab initio calculations of **S**-methyl-**N,N**-dimethylthiocarbamate. *Spectrochim. Acta* **1993**, *49A,* 2007-2026, https://doi.org/10.1016/S0584-8539(09)91012-1.
51. Michalska, D.; Wysokinski. R. The prediction of Raman spectra of platinum(II) anticancer drugs by density functional theory. *Chemical Physics Letters* **2005**, *403*, 211-217, https://doi.org/10.1016/j.cplett.2004.12.096.
52. Hassan, M.M.A.; Mohamed, M.E.; Mian, M.S. Analytical Profiles of Drug Substances, Naloxone Hydrochloride. **1985**, *14*, 453-489, https://doi.org/10.1016/S0099-5428(08)60588-2.
53. Mundhey, D.A.; Sapkal, N.P.; Daud, A.S. Simultaneous quantification of buprenorphine HCl and naloxone HCl by Vierordt'S method. *International Journal of Pharmacy and Pharmaceutical Sciences* **2016**, *8*, 101-107.
54. Chain, F.E.; Leyton, P.; Paipa, C.; Fortuna, M.; Brandán, S.A. FT-IR, FT-Raman, UV-Visible, and NMR spectroscopy and vibrational properties of the labdane-type diterpene 13-epi-sclareol, Spectrochim. *Acta Part A* **2015**, *138*, 303-313, http://dx.doi.org/10.1016/j.saa.2014.11.049.
55. Bruno, T.J.; Svoronos, P.D.N. *CRC Handbook of Basic Tables for Chemical Analysis*. Second Edition, CRC Press, Taylor & Francis Goup, Boca Raton, 2011.

6. ACKNOWLEDGEMENTS

This work was supported with grants from CIUNT Project Nº 26/D608 (Consejo de Investigaciones, Universidad Nacional de Tucumán, Argentina). The author would like to thank Prof. Tom Sundius for his permission to use MOLVIB.